Living on the edge: Abric Pizarro, a MIS 4 Neanderthal site in the lowermost foothills of the southeastern Pre-Pyrenees (Lleida, Iberian Peninsula)

Sofia C. Samper Carro [a,b,c,*], Susana Vega Bolivar [c], Jezabel Pizarro Barbera [c], Eboni Westbury [a], Simon Connor [a,b], Ethel Allué [d,e], Alfonso Benito-Calvo [f], Lee J. Arnold [g], Martina Demuro [g], Gilbert J. Price [h], Jorge Martinez-Moreno [c], Rafael Mora [c]

[a] School of Culture, History and Language, College of Asia and the Pacific, Australian National University, Australia
[b] ARC Centre of Excellence for Australian Biodiversity and Heritage, Australian National University, Australia
[c] Centre d'Estudis del Patrimoni Arqueologic, Facultat de Lletres, Universitat Autónoma de Barcelona, Spain
[d] Institut Catala de Paleoecologia Humana i Evolucio Social (IPHES-CERCA), Spain
[e] Universitat Rovira i Virgili (URV), Departament d'Historia i Historia de l'Art, Spain
[f] Centro Nacional de Investigación Sobre la Evolución Humana (CENIEH), Paseo Sierra de Atapuerca 3, 09002, Burgos, Spain
[g] School of Physics, Chemistry and Earth Sciences, Environment Institute, and Institute for Photonics and Advanced Sensing (IPAS), University of Adelaide, North Terrace Campus, 5005, Adelaide, SA, Australia
[h] School of the Environment, The University of Queensland, Brisbane, Australia, 4072

ABSTRACT

Extensive research carried out during the last 30 years in the lowermost foothills of the Southern Pyrenees has revealed the significance of this area for studying Neanderthal lifestyle and settlement histories in the Iberian Peninsula. With a large number of cave and rock shelter sites, broad-ranging chronologies, and relatively well-known sedimentation rates and environmental conditions, this enclave continues to improve our knowledge about Neanderthal behaviour in Western Europe.

Here we present the chronostratigraphic, technological, faunal, and palaeoenvironmental results from Abric Pizarro, a recently discovered site from the region. Its archaeological sequence is centred on MIS 4, a poorly known period in Neanderthal history. The application of three different dating methods (newly obtained single-grain optically stimulated luminescence and U-series fossil teeth ages, in addition to previously published thermoluminescence ages) provides an accurate chronology for a site where the exceptional preservation of faunal remains leads to significant interpretations of Neanderthal hunting abilities and adaptability. Moreover, analysis of the lithic assemblage, as well as preliminary palaeoenvironmental data, are used to provide insights into the degree to which chronocultural or palaeoenvironmental factors were responsible for some of the significant differences observed among the four archaeological units explored in Abric Pizarro to date. Our results contribute to discussion about Neanderthal resilience and their livelihood before their disappearance from the archaeological record.

1. Introduction

Since the discovery of the first Neanderthal fossils in the 19th century, these hominins have been a sustained focus of study. Researchers have strived to identify anatomical and physiological similarities and differences between our closest relatives and anatomically modern humans (AMHs), their phylogenetic position, as well as suggesting

factors that contributed to their demise around 40ka years ago (e.g. Bailey and Lynch, 2005; Bocherens and Drucker, 2006; Banks et al., 2008; Churchill, 2014; Villa and Roebroeks, 2014; Agustí and Rubio-Campillo, 2017; Banks et al., 2021; Romagnoli et al., 2022; Gonzalez et al., 2023). This information has been mainly gained from archaeological deposits dated to the Last Interglacial cycles during the Late Pleistocene -MIS 5 (ca. 130-71ka) and MIS 3 (57-30ka)-. However,

to fully understand Neanderthal ways of life in the millennia before their extinction, further research is needed to characterize the preceding glacial maxima (MIS 4; 71-57ka), at both regional and local scales.

MIS 4 is generally characterized as a sub-continental scale glaciation over northern Europe, coupled with dry conditions in continental eastern Europe (Helmens, 2014). The ice volume maximum, centred at 65 ka, was preceded by a progressive increase in ice volume through MIS 5 and a decrease in summer insolation (e.g. Sánchez-Goñi, 2022). Although these global environmental conditions are relatively well-known from environmental records in central and northern Europe and the Levant, there are few site-specific palaeoclimatic proxies in the Iberian Peninsula and western Europe, with scarce data available to understand local environmental conditions in these regions during MIS 4 (Fig. 1). Nonetheless, research on glacial and fluvioglacial deposits in river valleys in NE Spain provide data to interpret glacial-interglacial cycles in this region from ca. 70ka onwards. In the Aragon Valley glacier, evidence from moraine M2 dated the Last Maximum Ice Extent (LMIE) around 68 ± 7 ka (García-Ruiz et al., 2013), also identified in the Cinca and Gállego Rivers and associated to a strong increase in fluvial discharge and sediments availability related to the transition to deglaciation (Peña et al., 2004; Lewis et al., 2009). Other nearby moraines also confirm evidence for a LMIE event in the central Pre-Pyrenees during the MIS 4 (Sancho et al., 2003, 2018; Turu et al., 2023).

Moreover, some recent reviews of palaeobotanical data from archaeological sites in the Iberian Peninsula include sites with records dating to MIS 4 located in mediterranean (Abric Romani and Abric Pastor) and Atlantic/Euro-siberian (Axlor) bioregions (Ochando et al., 2022; Revelles et al., 2022). In Abric Romaní (Capellades, Barcelona), there is a dominance of *Pinus* throughout the sequence, with a phase of climate warming identified around 70–67 ka, characterized by higher percentages of arboreal pollen and thermophilic taxa (evergreen *Quercus* and *Olea-Phillyrea*), This phase was interrupted by a period of cooling between 66 and 59ka characterized by an increase in steppic taxa (Poaceae and *Artemisia*), followed by an increase in meso and thermophilic taxa (e.g. Burjachs et al., 2012; Revelles et al., 2022). Multiproxy analyses conducted from the MIS 4 occupations at Abric del Pastor (Alcoy, Alicante) indicate a mosaic of biotopes, with predominantly cold

conditions (Connolly et al., 2019). In the site of Axlor (Biscay) in northern Spain, pollen studies indicate that during MIS 4, the landscape surrounding the site was dominated by grasses and heather, with patchy evergreen-boreal forest (Demuro et al., 2023).

In addition to pollen data from archaeological sites, the pollen cores extracted from the Padul wetland (Granada) and the Villarquemado palaeolake (Teruel) provide significant pollen reference sequences from mediterranean bioregions. The Padul 15-05 sediment core contains a continuous sedimentary and palaeoenvironmental record of the last ca. 200,000 ka, with two pollen zones attributed to MIS 4 (Zones 3a and 2c) (Camuera et al., 2019; Ochando et al., 2022). Zone 3a shows a decline in arboreal pollen relative to the previous zone, with an average of ca. 10% in *Quercus* total, with some peaks for *Alnus*, *Abies* and *Cedrus* (1.5%) and *Pinus* averaging 57%. There is a significant pollen change in Zone 2c (60-43ka), with relatively high Mediterranean forest values until ca. 51ka BP, when the last occurrence of *Abies* is recorded and *Pinus* show a similar average percentage as the previous zone (ca. 53%). An interesting ecological change from zone 3a to 2c at Padul is the loss of heathland taxa (Ericacea and Cistaceae) and their replacement with xerophytes (*Artemisia* and Amaranthaceae) (Camuera et al., 2019).

The Villarquemado core is an interesting case study to address palaeoenvironmental conditions in continental areas influenced by climatic extremes, similar to those observed in the southeastern Pre-Pyrenees. In Villarquemado, the pollen zone VIL-10 (71–57.5 ka) is characterized by the absence of Mediterranean taxa, with evergreen *Quercus* and *Juniperus* disappearing from the record, while aquatics and hygrophytes fluctuate, likely indicating intense environmental changes (González-Sampériz et al., 2020). This replacement of Mediterranean woody elements with mesophytic ones is similar to that observed in sites like Abric Romani, coupled with an abrupt contraction in *Juniperus* and an expansion of *Pinus* (Burjachs et al., 2012). Other persistent trees are deciduous *Quercus* at the beginning of the MIS 4 and cold-tolerant species such as *Betula* and *Alnus*. In general, the MIS 4 assemblage from Villarquemado suggests cold and relatively humid conditions (González-Sampériz et al., 2020). These local analyses remark the complexity of environmental responses to climatic changes observed in these sites, while highlighting gaps in our current knowledge about

Fig. 1. Map of the Iberian Peninsula with location of the sites mentioned in the text. 1) Abric Pizarro; 2) Estret de Tragó; 3) Cova Gran de Santa Linya; 4) Roca dels Bous; 5) Abric Romaní; 6) Arlampe; 7) Padul; 8) Villarquemado; 9) Lezetxiki; 10) Atxagakoa; 11) Covalejos; 12) Roca San Miguel; 13) Fuente del Trucho; 14) Fuente de San Cristóbal; 15) Moros de Gabasa; 16) Abric del Pastor, 17) Teixoneres; 18) Cova del Toll.

regional palaeoenvironmental conditions during MIS 4 in the Iberian Peninsula.

Focusing on Neanderthal subsistence, the few faunal assemblages documented in Iberian sites dated to the MIS 4 display a relatively wide range of species, with variations in the taxonomic representation likely to be related to the orographic location of the sites as well as biogeographic conditions (Fig. 1). In the north of the Iberian Peninsula, the fauna assemblages from levels B, C and D (50.7 ± 3.5–70.4 ± 5.3ka) of Axlor (Biscay) show a diversified fauna, with a progressive decrease of cervids, stability in the number of caprids (wild goat), and an increase in the number of large animals, especially equids (González et al., 2005; Demuro et al., 2023). In Arlampe (Biscay), faunal assemblages dated to the MIS 5/4 transition (70.6ka) are dominated by caprines (*Capra pyrenaica* and *Rupicapra pyrenaica*), low number of cervid remains, and no equids (Arceredillo et al., 2013; Rios-Garaizar et al., 2015). The faunal assemblage for level V from Lezetxiki (Gipuzkoa; 57 ± 2–70±9ka), disregarding the large number of ursids likely related to natural accumulations, yielded large numbers of *Cervus elaphus* remains, followed by *Bos/Bison* (Falguères et al., 2005; Lazuén and Altuna, 2012). In Atxagakoa (Biscay), deposits dated to MIS 4 show deer as the main taxon (Castaños et al., 2004; Yravedra and Cobo-Sánchez, 2015). In Covalejos cave (Cantabria), the faunal assemblage throughout the sequence is equally dominated by cervids (ca. 90%), with indicators of a specialisation for hunting juvenile individuals (Castaños, 2021). In the central plateau, chamois and ibex are represented from MIS 5 to MIS 3, with an increase in their representation after 70ka, although the presence of large bovids (*Bos/Bison*) and cervids is also recorded (e.g. Díez, 2007; Arceredillo and Díez, 2009; Yravedra and Cobo-Sánchez, 2015).

One of the reasons for the gaps in our knowledge about Neanderthal behaviour during MIS 4 is the scarcity of sites across the European continent dated to this period, which contrasts with the remarkable number of sites dated to MIS 5 and MIS 3. The limited number of MIS 4 sites has been attributed to population shrinkage, as well as a contraction and shift in the range of suitable habitats exploited by Western European Neanderthal populations (Stewart, 2005; Banks et al., 2021), although other factors, such as poor preservation of sites from this period should not be disregarded.

During the last few decades, research on several sites located in the Southern Pre-Pyrenees have revealed the significance of this region for studying Neanderthal lifestyles (Fig. 1). In the Pre-Pyrenees of Huesca, the oldest Neanderthal site yet identified consists of Roca San Miguel, with a chronology ranging from MIS6d to MIS5a, and evidence of site abandonment during the MIS 4 (Montes et al., 2021; Peña-Monné et al., 2021). In the same region, the younger sites of Fuente del Trucho (Mir and Salas, 2000; Montes et al., 2006), Fuentes de San Cristóbal (Rosell et al., 2000; Menéndez et al., 2009) and Gabasa (Montes et al., 2006; Santamaría et al., 2010) provide evidence of Neanderthal presence during MIS 3 (Fig. 1). In the Noguera county (Lleida), the earliest Neanderthal occupations documented comprise the lower units from Estret de Tragó, dated to the MIS 5 (130-90ka), followed by MIS 3 occupations documented in Tragó upper units, Roca dels Bous and Cova Gran de Santa Linya (Casanova et al., 2009; Martínez Moreno et al., 2010; Mora et al., 2011, 2018; de la Torre et al., 2012). Since 2007, field prospection programs have identified several other prehistoric and historical settlements in the eastern Pre-Pyrenees region (Pizarro et al., 2013). Among the new prehistoric sites identified, Abric Pizarro has yielded Middle Palaeolithic techno-complexes that indicate this site could contain occupations predating MIS 3, thereby representing a unique site for understanding the chronostratigraphy of Neanderthal presence in the southeastern Pre-Pyrenees.

An introduction to the geochronology and a preliminary analysis of the fauna and stone artefacts documented in the more recent archaeological units from Abric Pizarro was recently published (Vega Bolivar et al., 2018). However, validation of the site geochronology, as well as the development of new research lines, comprising palaeoenvironmental and biomolecular data, triggered new excavation seasons and analyses. Here we present the results from the new chrononometric and palaeoenvironmental data obtained from Abric Pizarro, as well as the preliminary analysis of the complete fauna and lithic assemblage from the site.

2. Material and methods

2.1. Site background

Abric Pizarro (X = 310819, Y = 4646877 UTM H31N ETRS89) is a rockshelter located 697 m asl, in an enclosed valley (Barranc de les Coves) at the foothills of the southeastern Pre-Pyrenees, near the villages of Vilamajor and Tartareu (Fig. 2). The site is located in a small cliff, 20 m above the valley bottom. The rockshelter dimensions are 35 m length, 4.3 m height and 6.4 m depth, with a sedimentary sequence of over 1.5 m depth (Vega Bolivar et al., 2018). In 2009, the excavation of a 1 × 4m trench demonstrated the archaeological potential of the site, with the first official excavation season conducted in 2010. Fieldwork seasons continued during non-consecutive years (2010–2013; 2016–2017).

Excavation revealed a lithostratigraphic sequence consisting of breccia, muds and conglomerates (Fig. 2C). Breccia are characteristic of the upper beds, which are composed of limestone clasts, boulders, and sandy mud matrix, suggesting formation processes related to the spalling and gravitational fall of the limestone host rock. Near to the wall and the ceiling, these beds are cemented by carbonate. Under the breccia upper beds, a mud layer appears associated with low energy and/or stagnant waters. The lower known sediments are boulders and breccia including lenses of sands and conglomerates made up of surrounded limestone pebbles. Thus, the lower sequence indicates the continuation of the limestone host rock degradation by gravitational processes, as well as water rills of significant energy.

Within this sequence, four archaeological units were identified (M, P, Q and S) based on the 3D location of every artefact, sedimentary element (i.e. rocks) and features (pits and hearths) documented (Fig. 3). This methodology permits the identification of discrete Neanderthal occupations, as sterile layers (i.e. without evidence of human occupation) separate the archaeological units (Martínez Moreno et al., 2016).

The complete assemblage from Abric Pizarro comprises over 29,062 3D-plotted items, including lithics and fauna, with more than 305,423 lithic and bone fragments smaller than 2 cm included in 'general bags' with an individual series of coordinates for each bag (Table 1). The extent of the excavated area for each different archaeological unit ranges from 27 sq. m in unit M to 2 sq. m in unit S (Table 1).

The existing chronological framework for the excavated sequence is based on thermoluminescence (TL) dating of two thermally altered chert artefacts from archaeological units M (sample MAD-5607BIN) and P (sample MAD-5605BIN). These chert samples yielded TL ages of 59.0 ± 5.4 ka and 62.6 ± 6.1 ka (1σ) for units M and P, respectively, which are centred around the MIS 4/3 transition and are consistent with a broader MIS 4 to early MIS 3 timeframe when considering their associated uncertainty ranges (Vega Bolivar et al., 2018).

New excavations were undertaken aimed at extending the excavated area to understand the horizontal distribution dynamics of the archaeological units M and P, as well as obtaining new dating material, palaeoenvironmental proxies, and bone fragments for palaeoproteomic analysis. The new ages, as well as the preliminary results from the fauna, stone artefacts and palaeoenvironmental proxies are presented here.

2.2. Methods

2.2.1. Geochronology

2.2.1.1. Single-grain optically stimulated luminescence (OSL) dating. Two OSL dating samples (samples PI17-2 and PI17-1) were collected from units P and Q to provide estimates of when the archaeological deposits
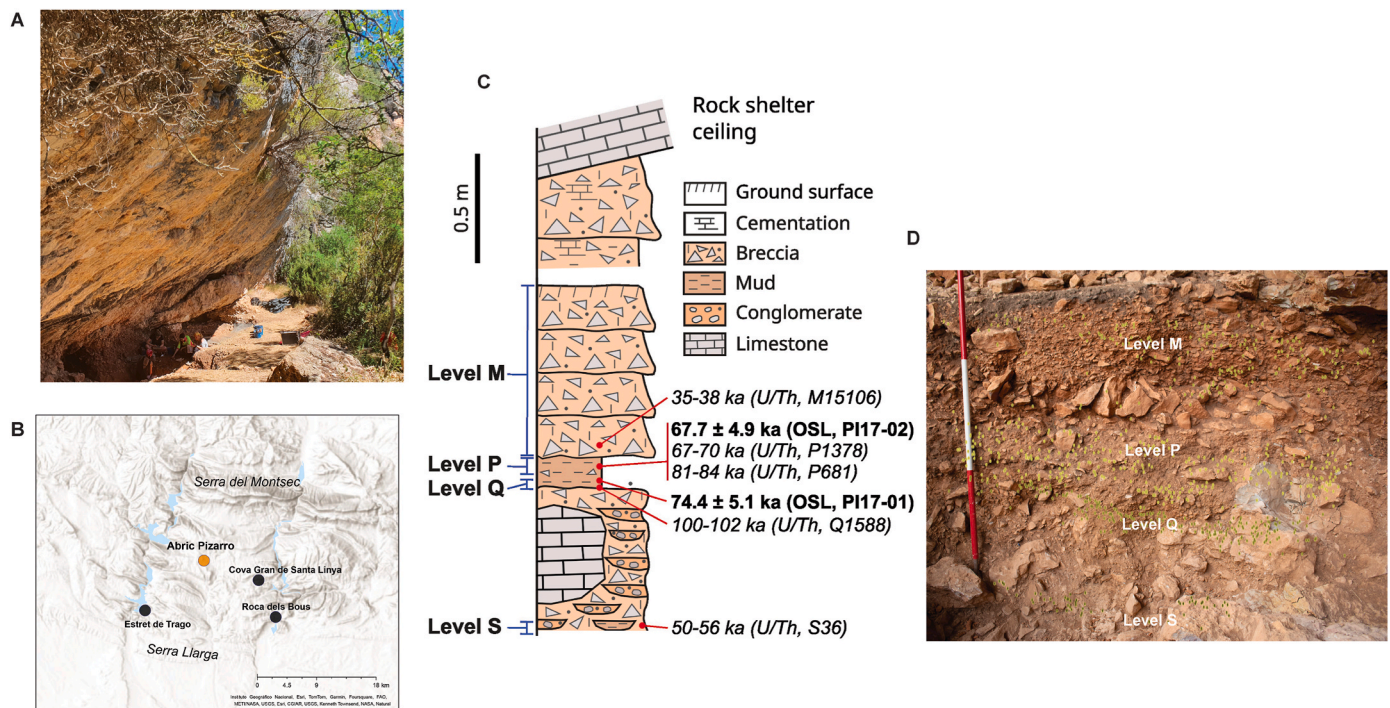
Fig. 2. A) General view Abric Pizarro rockshelter; B) Map of the area of study with nearby archaeological sites; C) Lithostratigraphic column of Abric Pizarro with approximated location of samples taken for OSL and U-Th new ages. Ground surface refers to the original surface of the deposit before excavation began. A description of the profile is provided in section 2.1. D) Photograph of the west section of the deposit, with vertical distribution of the archaeological units identified superimposed.

were last exposed to light prior to burial. OSL samples were taken from cleaned exposure faces using PVC or metal tubes and were immediately sealed in opaque plastic sheeting upon extraction. Additional sediment was collected from the immediate surroundings of each sample tube position for water content and dosimetry evaluations.

The samples were processed for single-grain quartz OSL analyses. Following initial wet sieving under low-level lighting in the CENIEH Luminescence Dating Laboratory, Spain, the samples were transferred to the University of Adelaide for further processing under safe light conditions (630 nm LEDs, <0.15 μW/cm^2 power density at sample position). The coarse-grain sieved fractions (180–250 μm) were treated with concentrated hydrogen peroxide (H_2O_2) and hydrochloric (HCl) acid to eliminate organics and carbonates, respectively. Quartz grains were then isolated using heavy liquid (LST lithium heteropolytungstate) density ranges of 2.62 g/cm^3 to 2.72 g/cm^3, and subsequently etched with 48% hydrofluoric acid for 40 min to remove the alpha-irradiated external layers. The etched grains were washed in 30% HCl to remove any precipitated fluorides and re-sieved using a 90 μm sieve to eliminate any disaggregated quartz grains and partially etched feldspars.

OSL measurements were made using the experimental apparatus, single-aliquot regenerative-dose (SAR) procedures, and quality assurance criteria published previously by Arnold et al. (2016, 2022), which are further detailed in the Supplementary Information.

The environmental dose rates for the single-grain OSL samples were estimated using a combination of *in situ* field gamma spectrometry and low-level beta counting, taking into account cosmic ray contributions (Prescott and Hutton, 1994), an assumed minor internal alpha dose rate (Bowler et al., 2003), beta dose attenuation and long-term water content (see Supplementary Information for further details).

2.2.1.2. Uranium-series dating. Uranium-series (U-Th) dating targeted fossil teeth excavated from every archaeological unit documented in Abric Pizarro. Fresh bone and teeth initially contain very small amounts of U but can become open systems for U-uptake after burial (Grün and McDermott, 1994). During the process of fossilisation, U migrates into apatites that scavenge U while excluding radiogenic Th. As the radioactive isotope ^{238}U undergoes alpha and beta decay, a series of short-lived nuclides such as ^{234}U, ^{234}Th, ^{230}Th are produced. By measuring the ratio of the daughter isotope ^{230}Th to its parent ^{238}U, a U-Th age can be calculated. In some situations, U uptake can be complex and occur at different rates and times after burial. Regardless of whether the uptake is rapid or progressive, and assuming no U loss through leaching after deposition, a U-Th date represents a minimum age for the fossil (Pike and Hedges, 2002). However, if U leaching occurs, it can distort the ratio of the daughter to parent isotope, leading to a maximum age for the fossil; this can sometimes lead to age overestimation (Sambridge et al., 2012). By analysing the concentration of U and conducting ^{230}Th age profiling through each tooth, the mode of U uptake and evidence of subsequent U loss in a given tooth sample can be determined and suitability for U-Th dating can be assessed (e.g., Price et al., 2021).

We employed a similar approach for collecting samples by drilling and obtaining powdered dentine along transects within the fossil teeth following procedures outlined in Price et al. (2013). Teeth were first cut with a diamond saw to expose the dentine and three separate sample powders from different loci in each fossil were collected (Fig. 4). These samples were analysed using a Nu Plasma HR multi-collector inductively coupled plasma mass spectrometer at the Radiogenic Isotope Facility (The University of Queensland, Brisbane, Australia) following the procedures described in Zhou et al. (2011).

2.2.2. Palaeoenvironmental data

Palynological sampling took place at two locations in the rock shelter – near the drip line and near the rock wall (Fig. 5). This was to gauge spatial variation in pollen composition and preservation. At each location, contiguous samples were collected from a vertical profile by first scraping back the trench wall to remove potential contamination. Samples 60–220 g in weight were then removed with a cleaned spatula and placed in sterile plastic bags. The vertical position and spatial
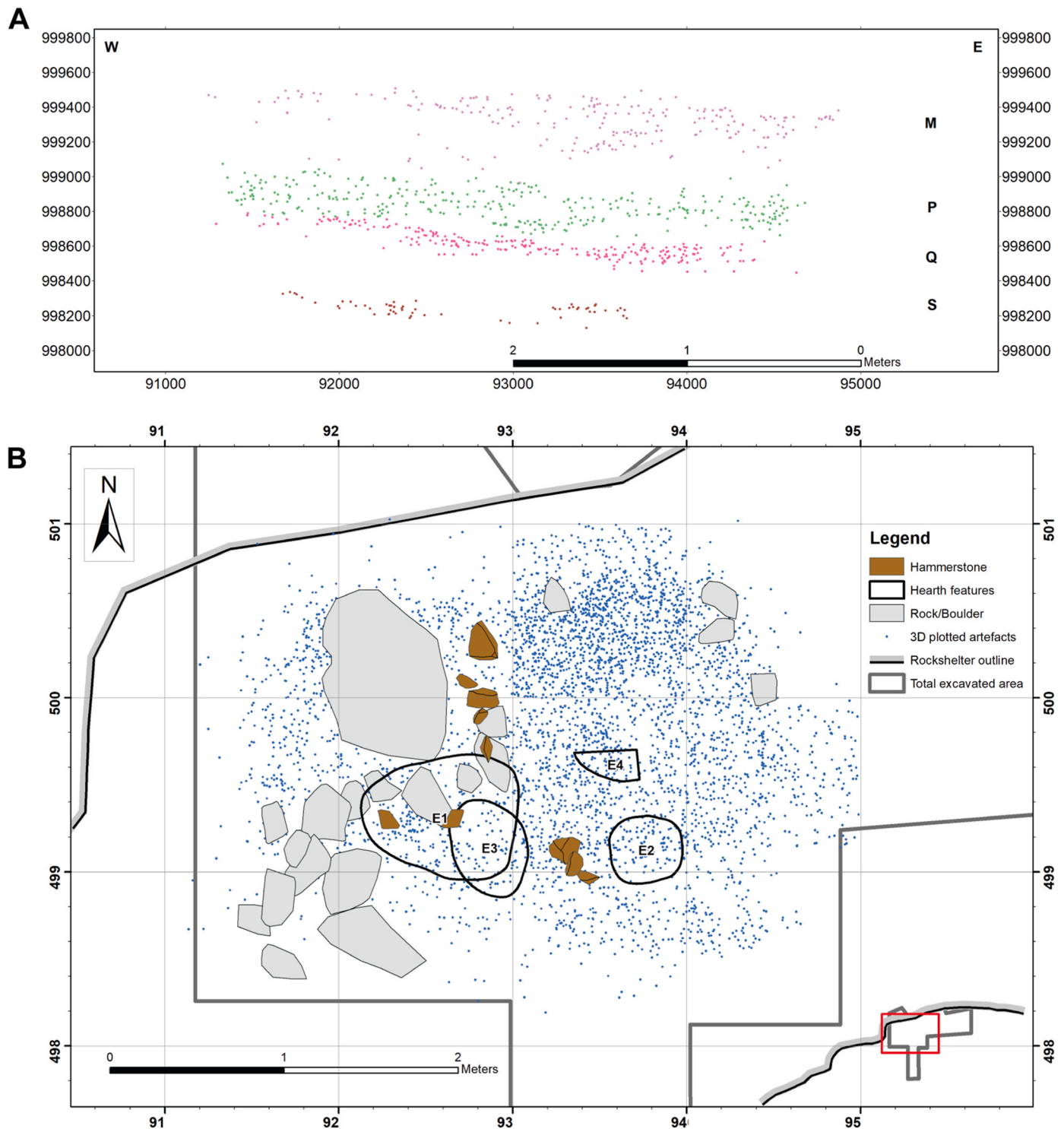
Fig. 3. A) Vertical distribution of the four archaeological units identified in Abric Pizarro based on the geometry of plotted materials (dots) and sterile layers separating each archaeological unit; B) General site map of archaeological unit Q, showing the horizontal dispersion of archaeological material in the excavated area, and hearths identified.

location of each sample were pinpointed using a total station. Vegetation surrounding the site was surveyed in 5 quadrats 20 × 20 m in size.

In the laboratory, samples of 5 ml volume were weighed and placed in 50 ml centrifuge tubes. Samples were saturated in 10% HCl to remove carbonates and spiked with exotic *Lycopodium* spores (9666 spores/ sample) to estimate pollen concentrations. Clay was deflocculated with 3% sodium hexametaphosphate and removed with repeated washes in distilled water. Much of the sediment matrix was resistant to chemical

treatment and was removed by repeated heavy liquid separation (LST, specific gravity 2.0). The remaining residues were subjected to 3 min of acetolysis and mounted in glycerol for pollen identification (Moore et al., 1991). Pollen was identified using the photographic guides of Reille (1992) and dichotomous key to Moore et al. (1991). Palynologists working on Neanderthal-aged pollen from the Pyrenees indicate how complex is to distinguish between *Olea* and *Phyllirea* pollen types due to morphological overlap (Revelles et al., 2022). These two pollen types

Table 1

Excavated surface, thickness of excavated archaeological units and number of 3D plotted fauna and lithics in per archaeological unit in Abric Pizarro. Abbr = NR: number of remains, including unidentified fragments and bone fragments identified to size-class (see 2.2.3 for further explanation of quantitative units); Cat: number of lithic artefacts classified to a technological category (see Table 6 for further details); NRt: Total number of remains, including fragments smaller than 2 cm in 'general bags'.

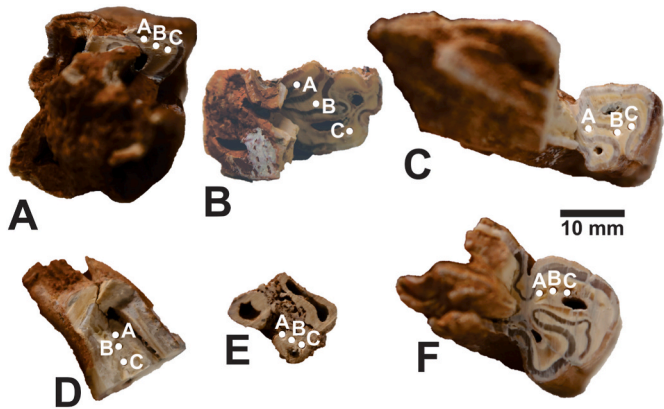| Archaeological unit	Excavated surface (sq. m.)	Archaeological unit thickness (cm)	Fauna (NR)	Lithics (cat)	NRt (fauna)	NRt (lithic)
M	27	30	8,448	8,185	169,741	25,493
P	14	17	1,742	4,523	86,652	16,888
Q	10	8	3,658	1,732	26,171	5,390
S	2	7	140	18	534	38
			13,988	14,458	283,098	47,809

Fig. 4. Tooth samples from Abric Pizarro for U-series dating showing sampling locations (A, B, C) for each tooth. See Table 3 for U-series isotopic data. A: Sample M15102 (*Equus ferus*, archaeological unit M) B: Sample M15106 (*Equus hydruntinus*, archaeological unit M) C: Sample P1378 (*E. hydruntinus*, archaeological unit P); D: Sample P681 (*E. ferus*, archaeological unit P); E: Sample Q1588 (*Capra pyrenaica*, archaeological unit Q); F: Sample S36 (*E. hydruntinus*, archaeological unit S).

were successfully distinguished in this analysis.

The charcoal remains at Abric Pizarro are not abundant. Due to their fragility sampling was carried out using hand picking. The studied assemblage is composed by 93 charcoal fragments from archaeological units M (15 fragments), P (47 fragments) and Q (31 fragments). The analysis was based on the identification of each charcoal piece observed under a reflected light microscope (Panthera Motic) with magnifications of ×50, ×100, ×200, ×500. For the identification each charcoal piece was fragmented with the hands to observe the three anatomical sections. To support the identification, we used the wood anatomy atlas of Schweingruber (1990).

2.2.3. Faunal analysis

The faunal assemblage documented in the four archaeological units excavated is housed at the Centre d'Estudis del Patrimoni Arqueologic (CeparqUAB) facilities. In this manuscript, we present an overview of the basic quantitative units calculated for the complete assemblage from Abric Pizarro. These units consists of the total number of fragments (NRt; including identified and unidentified specimens), number of remains (NR; including fragments identified to taxa and/or size/weight-class) and the number of identifiable specimens (NISP; comprising fragments identified to some taxonomic level). The size/weight-classes defined consider the range mass of the taxa identified in the assemblage (Saladié et al., 2011; Samper Carro et al., 2020).

Bone preservation was categorised based on the degree of weathering and splitting adapting the criteria proposed by Behrensmeyer (1978). Weathering stage 1 comprises fragments with scarce calcareous coating and light cracking; stage 2 was assigned to fragments with less than half of the cortical surface covered with calcareous coatings and initial splitting; stage 3 corresponds to heavily weathered fragments,
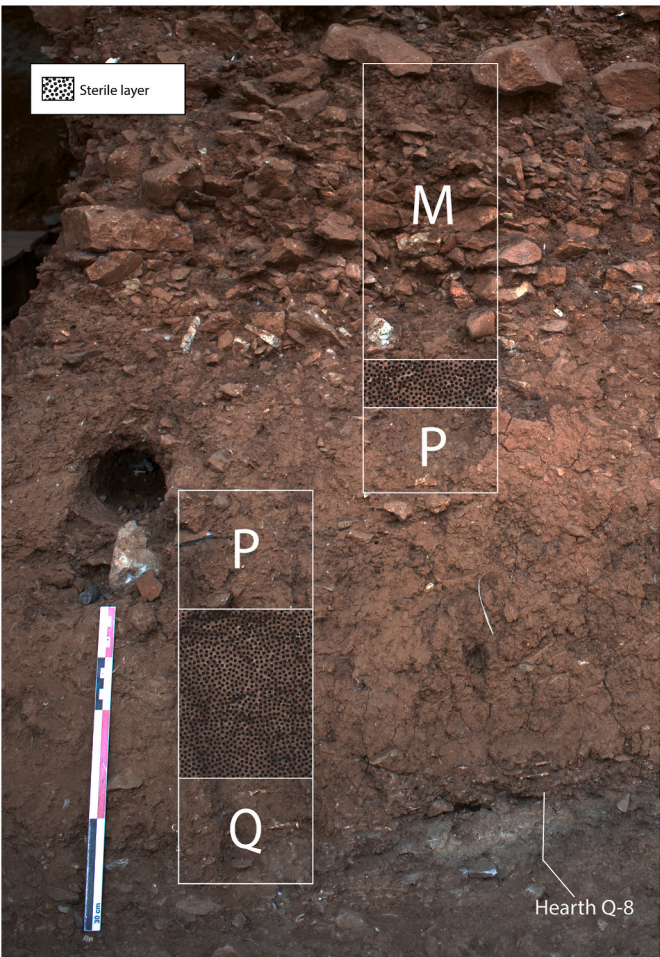

Fig. 5. Photograph showing the location where the pollen samples were collected from (white rectangles) and the correlation with the archaeological units identified and sterile (i.e. no cultural material recovered) phases.

where the cortical is missing, or completely covered with calcareous coatings. Abrasion was classified as stage 0 (unmodified), stage 1 (light abrasion), and stage 2 (rounded cortical and fracture edges). Bone colouring as accounted for no colour differences (stage 0), fragments with black-blue small spots (1), brown fragments (2), fragments displaying a black coloration (3), and fragments with a white-grey colour (4).

Anthropogenic and non-anthropogenic modifications were preliminary identified at the macroscopic level with a hand lens (10×). Anthropogenic modifications identified included butchery-related marks (incision and scrapes) and those related to intentional breakage (impact points, impact flakes, conchoidal and negative scars, percussion pits, percussion striae, peeling and indirect percussion (e.g. White, 1992; Capaldo and Blumenschine, 1994; Fisher, 1995; Pickering and Egeland, 2006). Nonanthropogenic modifications recorded comprise punctures,

gnawing, tooth marks and digestion damage (e.g. Fisher, 1995; Blumenschine et al., 1996; Pickering, 2002; Pante et al., 2012; Fernandez-Jalvo and Andrews, 2016). Bone fracture angles and outlines, and preserved shaft length and circumference were recorded following the criteria proposed by Villa and Mahieu (1991). As such, angles were classified as straight, oblique or irregular while outlines were described as transverse, spiral, orthogonal or mixed. Burning was identified by the presence of shrinking and/or cracking (Shipman et al., 1984; Nicholson, 1993; Stiner et al., 1995).

2.2.4. Stone artefact analysis

The analysis of the lithic assemblage followed *chaine opératoire* principles, where artefacts are defined following the spatial-temporal reduction knapping process (Lemonnier, 1983, 1993, 2010; Pelegrin et al., 1988; Boëda et al., 1990; Geneste, 1991; Audouze and Karlin, 2017; Audouze et al., 2017). This process integrates the different phases entailed in raw material selection, reduction knapping systems, and the distribution and discard of artefacts within the site.

Raw materials were characterized following previous lithographic analysis from a local and regional scale (Roy et al., 2013). The characterization of knapping systems focuses on the analysis of cores and retouched tools, as these categories show attributes to evaluate the techno-economical and techno-cognitive aspects (Boëda, 1990). These tool types are key to detect continuities and discontinuities in the technological sphere of prehistoric groups, favouring the identification of new technological traditions.

For the analysis of cores, we followed the criteria defined for Levallois and Discoid technological systems, characteristic of Middle Palaeolithic settlements (Boëda, 1990; 1993, 2005). We include the characterization of other expeditive reduction systems, which are usually considered secondary, but which play an important role in this site (Casanova i Martí et al., 2014). Retouched tools were analysed based on analytical typology principles (Laplace, 1972; Laplace and Saénz de Buruaga, 2020–2003), adding variations referring to the description of specific attributes.

Finally, we consider the spatial distribution and discard patterns based on the tridimensional position of the artefacts in the site to discuss sedimentation rates and occupation density. This approach allows us to consider archaeostratigraphic indicators to define the precise archaeological context of the artefacts (Mora et al., 2010, 2020; Martínez-Moreno et al., 2011; Roy, 2015).

3. Results

3.1. Chronological framework

3.1.1. Single-grain optically stimulated luminescence (OSL) dating

A summary of the single-grain OSL D_e values, dose rate data and final ages for the Abric Pizarro sediment samples is shown in Table 2, with the D_e distribution of each sample depicted as radial plots in Fig. 6. Both samples exhibit homogeneous D_e distributions characterized by low dose dispersion (relative D_e range = 2.1–2.2), D_e scatter that is reasonably well-represented by the weighted mean value (as indicated by the large proportions of grains lying within the 2σ grey bands), and overdispersion of 28 ± 2% to 32 ± 3% (Fig. 6). These overdispersion values are broadly similar to those reported for well-bleached and unmixed single-grain OSL D_e datasets (e.g., Arnold and Roberts, 2009; Hocknull et al., 2020; Arnold et al., 2022), including those from similar well-bleached depositional settings across the Iberian Peninsula (e.g. Arnold et al., 2016; Demuro et al., 2019, 2023; Zilhão et al., 2020, 2021; Daura et al., 2021; Rios-Garaizar et al., 2015). Neither D_e datasets are considered significantly positively skewed according to the weighted skewness test outlined by Bailey and Lynch (2005) and Arnold and Roberts (2011). Application of the maximum log likelihood (L_{max}) test (Arnold et al., 2009) indicates that the central age model (CAM) is statistically favoured over the three- or four-parameter minimum age models (MAM-3 or MAM-4) of Galbraith et al. (1999) for both datasets.

Collectively, these single-grain OSL D_e characteristics suggest that the samples do not suffer from major extrinsic D_e scatter related to insufficient bleaching prior to burial (e.g., Arnold et al., 2008, 2011), syn-depositional mixing with pre-existing rock shelter deposits prior to burial (e.g. Arnold et al., 2019; Zilhão et al., 2020; Ruiz et al., 2021), or widespread post-depositional sediment mixing between units (e.g., Arnold et al., 2012a, 2013). It seems likely that the low-to-moderate overdispersion observed for these samples is attributable to intrinsic experimental scatter not captured by the dose recovery test (e.g.

Table 2
Single-grain OSL dating results for the Abric Pizarro samples.

Sample	Unit	Grain size (μm)	Water content (%)[a]	Environmental dose rate (Gy/ka)				Equivalent dose (D_e) data				Age (ka)[f,j]
				Beta dose rate[b]	Gamma dose rate[c]	Cosmic dose rate[d]	Total dose rate[e,f]	No. of Grains[g]	Over-dispersion (%)[h]	Age model[i]	D_e (Gy)[f]	
PI17-2	P	180–250	2.1/15.0	1.54 ± 0.08	0.91 ± 0.05	0.02 ± 0.01	2.50 ± 0.15	122/2400	33 ± 2	CAM	169.0 ± 6.1	67.7 ± 4.9
PI17-1	Q	180–250	2.0/15.4	1.35 ± 0.07	0.80 ± 0.05	0.02 ± 0.01	2.19 ± 0.13	247/2000	28 ± 2	CAM	163.2 ± 3.6	74.4 ± 5.1

[a] Present-day water content/long-term estimated water content, expressed as % of dry mass of mineral fraction, with an assigned 1σ relative uncertainty of ±20%. The long-term water contents have been estimated as being equivalent to 40% of the present-day saturated water contents.

[b] Beta dose rates were calculated using a Risø GM-25-5 low-level beta counter (Bøtter-Jensen and Mejdahl, 1988), after making allowance for beta dose attenuation due to grain-size effects and HF etching (Mejdahl, 1979; Brennan, 2003). Radionuclide concentrations and specific activities of beta counting standards have been converted to dose rates using the conversion factors given in Guérin et al. (2011).

[c] Gamma dose rates were calculated from *in situ* measurements made at each sample position with a NaI:Tl detector using the 'energy windows' method detailed in Arnold et al. (2012b) and Duval and Arnold (2013). Radionuclide concentrations and specific activities of gamma spectrometry calibration materials, and K, U, Th concentrations determined from the field gamma-ray spectra have been converted to dose rates using the conversion factors given in Guérin et al. (2011).

[d] Cosmic-ray dose rates were calculated according to Prescott and Hutton (1994) and assigned a relative 1σ uncertainty of ±10%.

[e] Total dose rate includes an assumed internal alpha + beta dose rate of 0.03 Gy/ka for quartz, with an assigned relative 1σ uncertainty of ±30%, is based on intrinsic ^{238}U and ^{232}Th contents published by Mejdahl (1987), Bowler et al. (2003), Jacobs et al. (2006b), Pawley et al. (2008), and Lewis et al. (2020), and an a-value of 0.04 ± 0.01 (Rees-Jones, 1995; Rees-Jones and Tite, 1997). Intrinsic radionuclide concentrations and specific activities have been converted to dose rates using the conversion factors given in Guérin et al. (2011), making allowance for beta dose attenuation due to grain-size effects (Mejdahl, 1979).

[f] Mean ± total uncertainty (68% confidence interval), calculated as the quadratic sum of the random and systematic uncertainties.

[g] Number of D_e measurements that passed the SAR rejection criteria and were used for D_e determination/total number of D_e values analysed.

[h] The relative spread in the D_e dataset beyond that associated with the measurement uncertainties for individual D_e values.

[i] Age model used to calculate the sample-averaged D_e value for each sample: CAM = central age model (Galbraith et al., 1999).

[j] Total uncertainty includes a systematic component of ±2% associated with laboratory beta-source calibration.
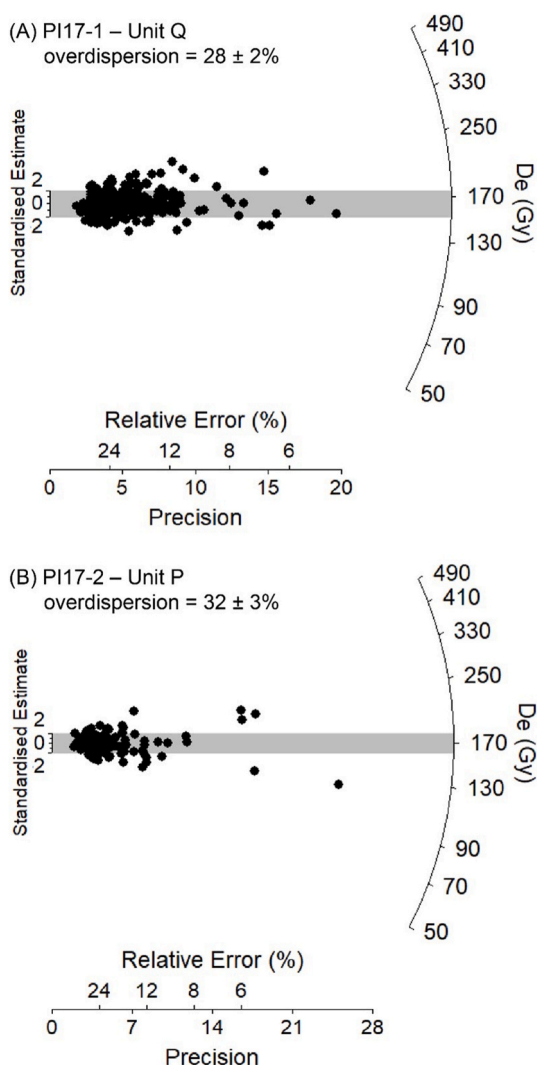
Fig. 6. Single-grain D_e distributions for the OSL dating samples, shown as radial plots. The grey bands on the radial plots are centred on the D_e values used for the age calculations, which were derived using the central age model (CAM). Individual D_e values that fall within the shaded region are consistent with the CAM burial doses used for age calculation.

Galbraith et al., 2005; Jacobs et al., 2006a,b; Demuro et al., 2013; Arnold et al., 2013) and extrinsic field-related scatter associated with beta-dose spatial heterogeneity (e.g. Nathan et al., 2003; Arnold et al., 2014; Martin et al., 2015; Smedley et al., 2020). The single-grain OSL ages for these samples have therefore been obtained using the weighted mean (CAM) D_e estimate, in accordance with their L_{max} test results (Arnold et al., 2009) (Table 2).

Sample PI17-2 from Unit P yields a single-grain OSL age of 67.7 ± 4.9 ka, while sample PI17-1 from the underlying Unit Q provides an age of 74.4 ± 5.1 ka (1σ). These two OSL ages are stratigraphically consistent with each other, and in agreement with the previously obtained TL ages of 59.0 ± 5.4 ka and 62.6 ± 6.1 ka for Units M and P, respectively (Vega Bolivar et al., 2018). Taken together, the independently derived TL and OSL ages provide good support for the reliability of luminescence dating at this site. The combined luminescence chronology reveals that archaeological units P, Q and M most likely accumulated during MIS 4 (71–57 ka; Lisiecki and Raymo, 2005), with the 2σ uncertainty ranges of Units M and P encompassing the start of MIS 3 (57–29 ka) and the 2σ uncertainty ranges of Units P and Q overlapping with the end of MIS 5 (130–71 ka).

3.1.2. U-Th dating

We produced 18 U-Th ages (Table 3) for six teeth from the deposit (three dates per tooth). With the exception of one tooth, sample S-36, U concentration is generally homogenous across the dentine portion of each individual tooth. Similarly, the ^{230}Th ages are also consistent within the dated specimens including some within individual teeth that are statistically indistinguishable. For tooth S-36, the resulting ^{230}Th ages are also consistent with each other despite one magnitude of difference in apparent U concentration; the variation in U concentration is most likely a result of an error manually weighing the very small samples (typically <8 mg), but it is important to note that this does not affect the final age (see also Price et al., 2021). Taken together, the consistency between U concentration and ages within individual teeth suggests that each one has produced reliable minimum ages and there is no evidence for U leaching. We interpret these minimum ages as: sample 15102 (unit M) at ca. 35–37 ka, sample 15106 (unit M) at 35–39 ka, sample 1378 (unit P) at ca. 68–70 ka, sample 681 (unit P) at ca. 82–85 ka, sample 1588 (unit Q) at ca. 101–103 ka, and sample 36 (unit S) at 51–56 ka.

3.2. Palaeoenvironmental proxies

Palynological samples collected near the rock shelter wall proved to have excellent pollen preservation while the samples near the drip line had low pollen concentrations. Results from the former are presented here (Fig. 7). In the 6 samples analysed to date, ranging from archaeological units Q, P and M, the pollen assemblages are dominated (46–66%) by evergreen oak (*Quercus ilex/coccifera*-type pollen). Other important components are *Olea*, *Phillyrea*, *Juniperus*, *Pistacia* and *Pinus*, typical of Mediterranean vegetation. Pollen of mesic trees occurs at low frequencies (e.g. *Betula, Castanea, Fraxinus, Corylus, Juglans, Quercus* deciduous-type). Tree and shrub pollen dominates the record (>87%). Herb pollen types are diverse but their overall percentages are low (<13%), with Poaceae and Amaranthaceae the most important taxa. Aquatic pollen types and non-pollen palynomorphs were scarce.

The assemblages do not vary greatly between archaeological periods. There appears to be more *Pinus* and less *Quercus* and Poaceae in the lowermost unit, Q. Samples from middle unit P have somewhat more *Juniperus*, apart from the uppermost sample from this unit, which is highly enriched with *Olea* and *Phillyrea* pollen. Unit M samples have more *Quercus* evergreen and Poaceae and somewhat less Amaranthaceae, but the differences between the three units are unlikely to be significant. The overall picture is of evergreen oak dominance.

The analysis of the 93 charcoal fragments reveals that they correspond to the *Pinus sylvestris* type, undetermined conifers, and undetermined fragments (Table 4). Among these, *Pinus sylvestris* type is the only taxon identified in the assemblage. This taxonomic category encompasses three montane criophillous pines: *Pinus nigra* ssp. *salzmannii* (black pine), *Pinus sylvestris* (Scots pine), and *Pinus uncinata* (mountain pine). The wood anatomy of these three species does not allow differentiation. The wood anatomy of this taxon is characterized by a transverse section displaying resin canals, a radial section with fenestriform pits in the cross fields and dentate transverse tracheids, and a tangential section with uniseriate rays. *Pinus uncinata* often exhibits very narrow tree rings, which are indicative of environmental adaptation to cold conditions (Euba, 2008). However, this characteristic can also be observed in *Pinus sylvestris* growing under extreme cold conditions.

In the Iberian Peninsula, montane pines are typically found at the highest elevations in the south and in northern mountainous regions. In northeastern Iberia, *P. nigra* grows between 500 and 800 m asl., *P. sylvestris* between 1000 and 1700 m asl., and *P. uncinata* above 1800 m asl. (Folch and Natural, 1986; Blanco et al., 1998; Roiron et al., 2013). *Pinus sylvestris* is the most prevalent pine species in this region, while *P. uncinata* and *P. nigra* are less commonly found due to their specific ecological requirements (Folch and Natural, 1986).

Table 3

U-series isotopic concentrations for dated teeth from Abric Pizarro. See Fig. 4 for photos of dated teeth and sampling loci.

Unit	Sample	U (ppm) ±2s	^{232}Th (ppb) ±2s	(^{230}Th/^{232}Th)	(^{230}Th/^{238}U)	(^{234}U/^{238}U)	uncorr. ^{230}Th Age (ka)	corr. ^{230}Th Age (ka)	corr. Initial (^{234}U/^{238}U)
M	15102-A	31.41 ± 0.008	14.51 ± 0.02	1986 ± 5	0.302 ± 0.001	1.049 ± 0.001	37.0 ± 0.1	37.0 ± 0.1	1.054 ± 0.001
	15102-B	36.16 ± 0.013	2.35 ± 0.02	13393 ± 136	0.287 ± 0.001	1.045 0.001±	34.9 ± 0.1	34.9 ± 0.1	1.050 ± 0.001
	15102-C	41.78 ± 0.014	1.94 ± 0.02	18767 ± 168	0.287 ± 0.001	1.041 0.001±	35.1 ± 0.1	35.1 ± 0.1	1.045 ± 0.001
M	15106-A	31.68 ± 0.012	359.36 ± 0.45	82.8 ± 0.2	0.309 ± 0.001	1.029 ± 0.001	39.0 ± 0.1	38.7 ± 0.2	1.033 ± 0.001
	15106-B	33.09 ± 0.010	33.82 ± 0.06	925 ± 4	0.312 ± 0.001	1.042 ± 0.001	38.7 ± 0.2	38.7 ± 0.2	1.047 ± 0.001
	15106-C	39.96 ± 0.022	9.57 ± 0.03	3593 ± 18	0.284 ± 0.001	1.028 ± 0.001	35.2 ± 0.2	35.2 ± 0.2	1.031 ± 0.001
P	1378-A	29.30 ± 0.011	43.47 ± 0.09	1046 ± 3	0.511 ± 0.001	1.096 ± 0.001	67.9 ± 0.3	67.9 ± 0.3	1.116 ± 0.001
	1378-B	31.71 ± 0.012	32.14 ± 0.06	1558 ± 7	0.520 ± 0.002	1.100 ± 0.001	69.1 ± 0.4	69.1 ± 0.4	1.122 ± 0.001
	1378-C	25.18 ± 0.010	5.50 ± 0.02	7288 ± 34	0.525 ± 0.001	1.099 ± 0.001	70.1 ± 0.3	70.1 ± 0.3	1.121 ± 0.001
P	681-A	6.56 ± 0.003	113.79 ± 0.13	103.2 ± 0.4	0.591 ± 0.002	1.085 ± 0.001	84.7 ± 0.5	84.2 ± 0.6	1.109 ± 0.002
	681-B	7.23 ± 0.004	33.60 ± 0.04	386 ± 1	0.591 ± 0.002	1.082 ± 0.001	85.1 ± 0.5	85.0 ± 0.5	1.105 ± 0.001
	681-C	7.31 ± 0.004	13.87 ± 0.02	914 ± 3	0.572 ± 0.002	1.077 ± 0.001	81.7 ± 0.4	81.6 ± 0.4	1.097 ± 0.001
Q	1588-A	16.14 ± 0.010	461.05 ± 0.53	77.1 ± 0.2	0.726 ± 0.002	1.176 ± 0.001	101.4 ± 0.5	100.7 ± 0.5	1.236 ± 0.001
	1588-B	21.96 ± 0.008	5.09 ± 0.02	9603 ± 39	0.733 ± 0.002	1.181 ± 0.001	102.4 ± 0.5	102.4 ± 0.5	1.242 ± 0.001
	1588-C	20.69 ± 0.007	17.45 ± 0.03	2663 ± 7	0.740 ± 0.002	1.188 ± 0.001	102.8 ± 0.4	102.8 ± 0.4	1.251 ± 0.001
S	36-A	22.35 ± 0.006	3.74 ± 0.01	8142 ± 30	0.449 ± 0.001	1.107 ± 0.001	56.3 ± 0.2	56.3 ± 0.2	1.125 ± 0.001
	36-B	2.90 ± 0.001	1.00 ± 0.01	3861 ± 13	0.438 ± 0.001	1.100 ± 0.001	54.9 ± 0.2	54.9 ± 0.2	1.117 ± 0.001
	36-C	18.1 ± 0.005	14.70 ± 0.02	1535 ± 4	0.411 ± 0.001	1.100 ± 0.001	50.6 ± 0.1	50.6 ± 0.1	1.115 ± 0.001

Note: Ratios in parentheses are activity ratios calculated from the atomic ratios but normalised to measured values of secular-equilibrium HU-1 (Ludwig et al., 1992). Errors are given at the 2σ level. ^{230}Th ages are calculated using Isoplot EX 3.0 (Ludwig, 2003) with decay constants λ238 = 1.551 × 10-10 yr-1 (for ^{238}U), λ234 = 2.826 × 10-6 yr-1 (for ^{234}U) and λ230 = 9.158 × 10-6 yr-1 (for ^{230}Th), respectively (Cheng et al., 2000). 2σ errors in the uncorrected (uncorr.) ages were propagated directly from the uncertainties in the (^{230}Th/^{238}U) and (^{234}U/^{238}U). The corrected (corr.) ^{230}Th age was calculated using the assumed bulk earth or upper crust value equivalent to the detrital ^{230}Th/^{232}Th activity ratio of 0.83. See Zhou et al. (2011) for a detailed description of the analytical protocol used.

3.3. Faunal analysis

The complete faunal assemblage from Abric Pizarro comprises over 280,000 bone fragments (NRt; Table 1). The large quantity of unidentified fragments smaller than 2 cm (average 94%) indicates the high fragmentation rates of the assemblage, as well as the integrity of the deposit in terms of preservation of small bone fragments. A total of 13,988 specimens were identified to taxa or size/weight class. A detailed taphonomic analysis of the faunal assemblages from the units M and P has been published elsewhere (Westbury et al., 2024). The results presented here provide a general overview of the taxonomic composition and bone preservation stages of the complete faunal assemblage.

The taxonomic composition in the site consists of a diverse fauna, with variations between archaeological unit (Fig. 8). Unit S yielded remains of small and medium-sized herbivores, with a larger relative abundance of cervids, and over 30% of equids and large size animals. The percentage of large bovids (*Bos/Bison* sp.) decreases dramatically throughout the sequence, with small-sized herbivores and caprinae (*Capra pyrenaica*) dominating the assemblage in unit Q, followed by cervids and medium-sized herbivores. Conversely, over 50% of the fauna from units P and M consists of cervids and medium-sized herbivores, with more equids than caprinae but a larger number of small-sized than large herbivores. Diversity indices for common herbivore prey (i.e. bovids, cervids, equids) do not show dominance of a species or herbivore size in any of the units, with a higher diversity in units S and Q

based on the results of Simpson (1-D) and Shannon (H) indices (1-D M = 0.78, P = 0.78, Q = 0.84, S = 0.85; H M = 1.64; P = 1.64; Q = 1.87; S = 1.92). Nevertheless, sample size needs to be considered, as it has been demonstrated to affect calculations of taxonomic diversity (Neeson et al., 2013). With large differences in the number of remains identified in each archaeological unit, taxonomic diversity and composition would need to be reassessed in future studies (see also Westbury et al., 2024).

The number of remains assigned to wild boar (*Sus scrofa*) and Rhinocerontidae is scarce, with carnivores only present in unit M by low numbers (Table 5). Lagomorphs (*Oryctolagus cuniculus* and *Lepus aeropaeus*) are more abundant in unit Q compared to the other units, although further analysis is required to confirm this hypothesis. A remarkable difference is the presence of pond turtle (*Mauremys leprosa*) in the upper units, with higher number of remains in unit M than P and absent in the lower units (Table 5).

Bone preservation is characterized by good integrity of bone cortical surfaces, with moderate splitting and carbonate coating. Less than 1% of the assemblages display evidence of abrasion, polishing or rolling. A higher number of bone fragments (>50%) with brown coloration were recorded in units M and P, with 14% and 9% of the fragments displaying this coloration in units Q and S respectively.

There is a significant difference on the percentage of burnt bones recovered in the different archaeological units analysed. Only 1% of the fragments documented in unit S display burning damage, while the percentage increases significant for unit Q (ca.26%) and then decrease
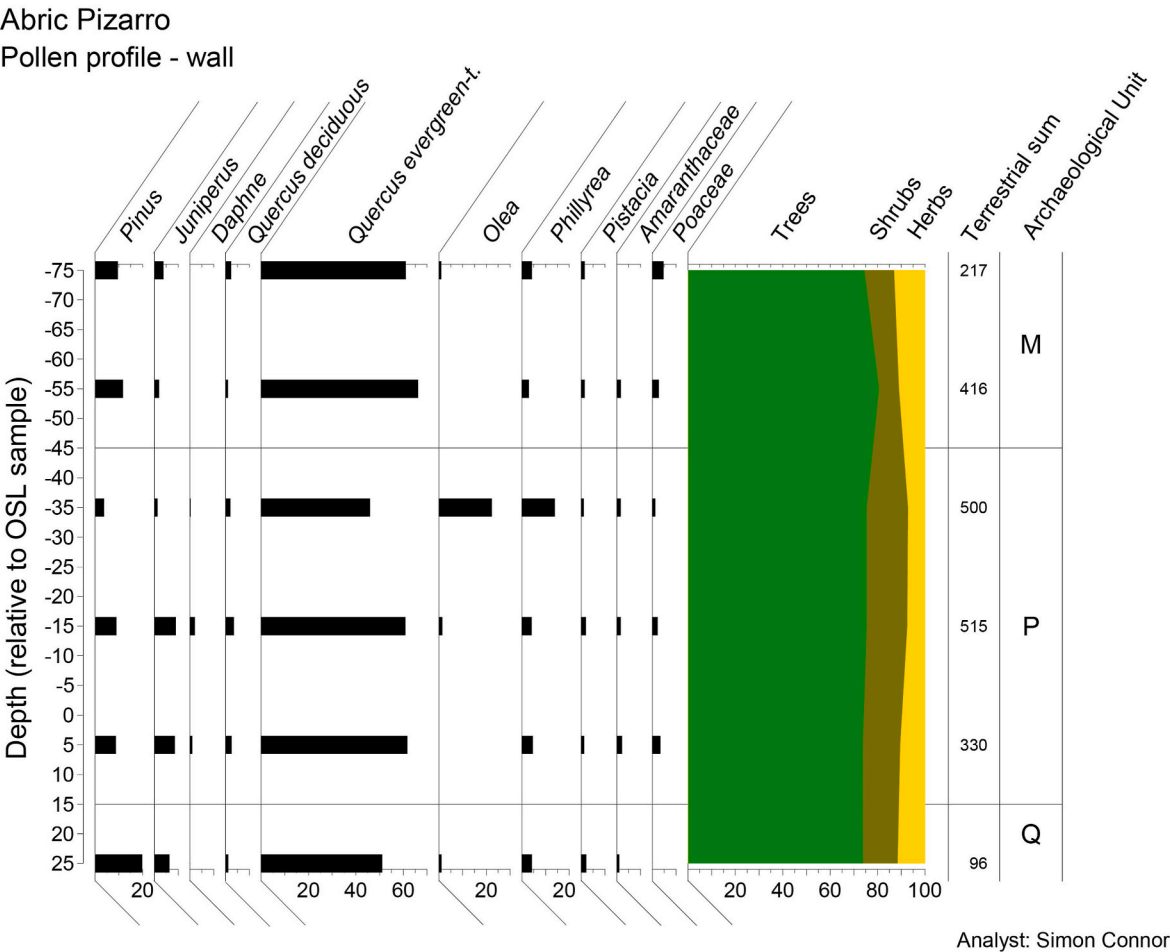
Fig. 7. Summarised pollen diagram.

Table 4
Results of the anthracological analyses from Abric Pizarro.

Taxa	Unit M	Unit P	Unit Q
Pinus tipus sylvestris	8	18	11
Undetermined conifer	3	8	6
Undetermined	4	21	14
Total	**15**	**47**	**31**

to ca.12% in units P and M. Human bone modifications are documented throughout the sequence, comprising incisions, scrapes, and percussion damage indicators.

3.4. Lithic analysis

The Abric Pizarro assemblage consist of 14,433 stone artefacts, distributed unevenly between units and categories, with these differences likely related to excavated surface and unit thickness (Table 6).

Chert is the most abundant raw material in every unit (99%), obtained from Garumnian outcrops (Roy et al., 2013). Regarding syn-/post-depositional processes, a large proportion of the assemblage (82%) is affected by desilication and patination, as well as carbonate coatings on the artefact surface. No evidence of water rolling or abrasion has been identified. Thermal alterations were recorded in 31% of the material, indicating the presence of hearths that were not identified *in situ*.

Of the 192 cores documented, 53% comprise core fragments, which have not been further considered to characterize knapping methods. Unit M is characterized by the adoption of Levallois Centripetal

Recurrent (LCR) methods (Boëda, 1993), while in units P and Q the predominant knapping method is Bifacial Centripetal Hierarchical. This method presents common attributes with the LCR and discoid methods, resulting in cores and blanks that are similar morphologically (Casanova i Martí et al., 2014; Bustos Perez et al., 2023). These preliminary observations indicate differences between the knapping systems adopted during the Unit P and Q occupations (centred on the first half of MIS 4 and potentially encompassing the MIS 5/4 transition at 2σ) and the Unit M occupation (centred on late MIS 4 and potentially spanning the MIS 4/3 transition at 2σ).

The analysis of the retouched tools indicated the selection of large size blanks (>5 cm length) with simple retouch, with a larger proportion (38%) of side scrapers (*racloirs*) than denticulates (14%). There is also evidence of abrupt retouch on notches and denticulates (Fig. 9). The most abundant morphologies in unit M are side scrapers with continuous retouch, with a larger number of artefacts with lateral retouch, although transversal and bilateral retouched tools are also identified. A characteristic of unit M is the presence of points, comprising 5% of the retouched tools. In units P and Q, the most common tools are notches and denticulated with lateral retouch.

4. Discussion

The new chronometric data, as well as the preliminary results from the palaeoenvironmental, zooarchaeological and techno-economic analyses, place Abric Pizarro as a significant site to investigate Neanderthal resilience during MIS 4, a poorly represented period characterized by harsh environmental conditions. Previously, this area had been
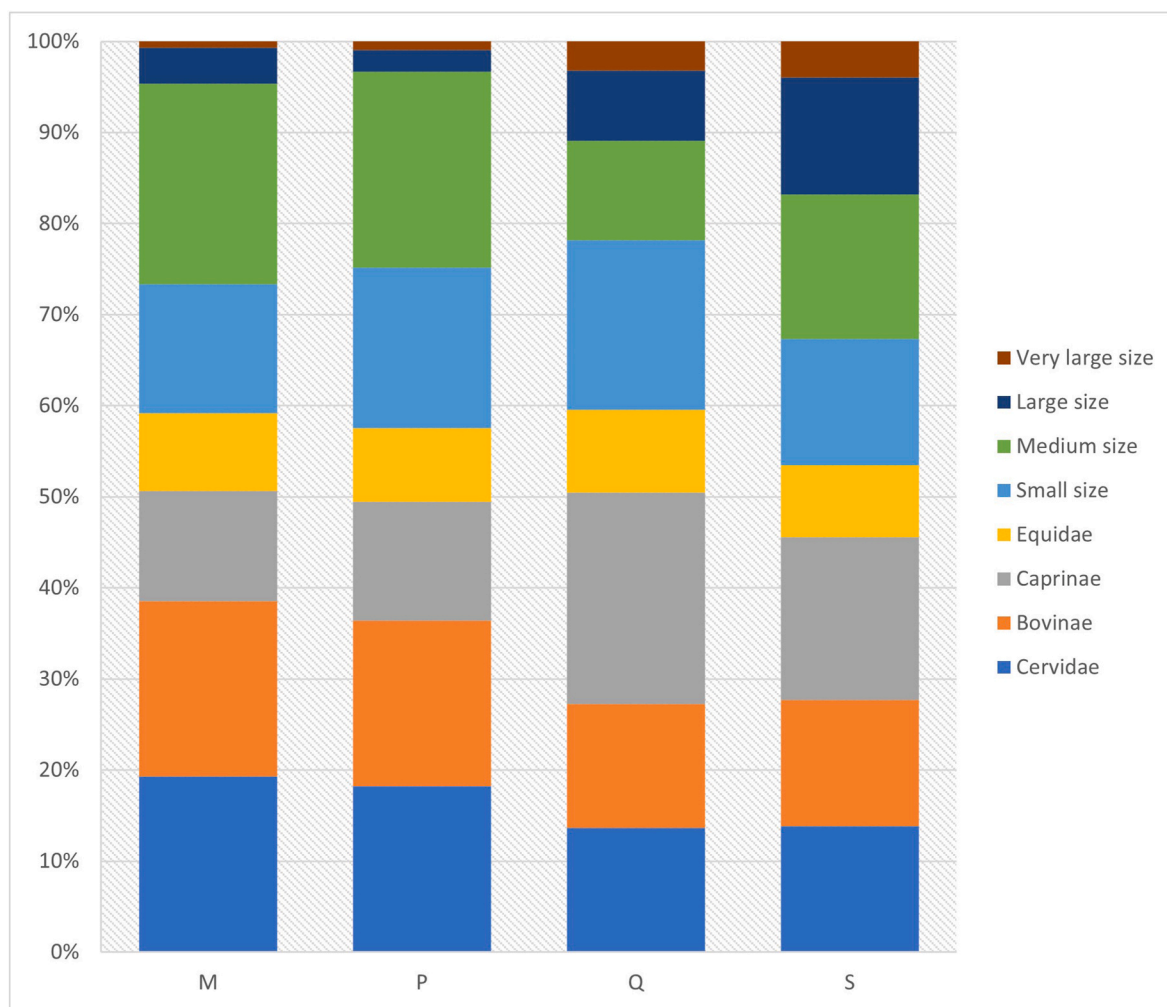
Fig. 8. Relative abundance of vertebrate remains in the four archaeological units analysed in Abric Pizarro.

considered unsuitable for stable and continuous Neanderthal presence during MIS 4 due to millennial-scale climatic shifts, which would have translated into extreme arid conditions with sharp temperature falls (d'Errico and Sánchez-Goñi, 2003).

The new chronometric ages reported for Abric Pizarrro support the identification of successful Neanderthal settlements in western Europe during the MIS 4. While the previous thermoluminescence dates and the new age estimations obtained from OSL and U-Th methods are in broad agreement with each other, there are some discrepancies regarding the U-Th ages that should be further discussed. The young ages obtained for the bottom of the sequence (unit S, sample S36, 50–56 ka) could be correlated to differences in apparent U concentration likely related to issues during laboratory processing (see comments in section 3.1.2). Nevertheless, these ages represent minimum estimates, suggesting delayed uptake of U in the sample. On the other hand, sample Q1588 (unit Q) produced a U-Th minimum age of 100–102 ka, implying at least a MIS 5 date for this unit, while the OSL age recovered from higher in the sequence is spanning the MIS 4/5 transition (74.4 ± 5.1 ka). This might suggest a fast sedimentation rate towards the bottom of the unit. Nevertheless, these differences support the need of further dating of the site, including different dating methods such as Uranium-Electron Spin Resonance (U-ESR) to refine the chronological relationships towards the base of unit Q and the underlying unit S. Additionally, for the topmost part of the sequence, radiocarbon dating applying the latest ultrafiltration protocols for purified bone gelatine (e.g. Higham et al., 2006), could increase the chronometric resolution of unit M.

Preliminary palynological results from Abric Pizarro provide insights

into the degree to which the Iberian Peninsula was affected by glacial conditions recorded elsewhere in central and northern Europe. The signals of glacial conditions in the Abric Pizarro pollen samples are quite subtle, a common situation in peninsular settings acting like refugia, with the occurrence of *Artemisia*, *Astragalus*-type and Amaranthaceae indicative of steppic vegetation. However, the low frequencies of these taxa in relation to the overwhelming dominance of evergreen oak pollen suggests that steppe vegetation did not occur near the study site, which itself was surrounded by dense evergreen oak woodland with other Mediterranean elements like juniper, *Olea/Phillyrea*, *Daphne* and *Pistacia*.

Remarkably, the preliminary palynological results from Abric Pizarro yielded exceptionally low percentages of pine pollen compared to other records from the region (Revelles et al., 2022). The high percentage of oak pollen in Abric Pizarro coincides with the palynological records published from Teixoneres and Cova del Toll (Fig. 1), interpreted as evidence of a thermophilus forest refugium in the region during the MIS 4-MIS 2 interval (Ochando et al., 2020a, 2020b). The palynological results from Abric Pizarro sets it apart from other comparable sites such as Abric Romani, where much higher percentages of conifers or grass pollen were observed, indicative of cooler forest or steppic conditions around those sites (Revelles et al., 2022). Together, the differences in pollen assemblages between sites point to a diverse and patchy landscape during the period of interest, one in which a wide variety of resources were present within a relatively small geographic area.

We anticipate that further chronometric and palaeoecological

Table 5

Faunal assemblage from Abric Pizarro. For abbreviations, see methods section.

	M	P	Q
Bos sp	16	7	2
Capreolus capreolus	9	1	
Rupicapra rupicapra	4		
Capra pyrenaica	14	4	29
Caprine	201	51	
Cervus elaphus	419	72	30
Cervidae	837	158	
Equus ferus	186	31	20
Equus hydruntinus	160	15	
Equus sp.	213	57	
Sus scrofa	6	3	1
Rhinocerontidae	3	1	
Ursus sp	6		1
Canis sp.	1		
Vulpes vulpes	1		
Hyenidae	2		
Lynx pardinus	1		
Felidae	1		
Carnivore	6		
Oryctolagus cuniculus	47	55	2742
Lepus europaeus	12	3	
Lagomorpha	154	75	
Rodentia	4		
Talpa europae	1		
Aves sp.	1		
Testudinidae	199	35	
Herbivore 1	214	154	41
Herbivore 1/2	717	69	
Herbivore 2	1184	248	24
Herbivore 2/3	260	25	
Herbivore 3	189	21	17
Herbivore 3/4	70	9	
Herbivore 4	46	12	7
Herbivore 5	1		
Undefined mammal	1404	237	39
Undefined ungulates	144	4	
Unidentified	1781	27	111
Unidentified <2 cm	152962	83599	22411
NISP	4965	973	172
NR	8514	1374	3064
NRt	161476	84973	25475
%NR	5.2726	1.61698	12.03
%NISP	58.316	1.14507	0.675
%NRt(2 cm)	94.727	98.383	87.97

Table 6

Technological categories documented in the different archaeological units, including excavated surface (m2) and average unit thickness.

Technological categories	M	P	Q	S	Total
Core	130	51	11		192
Retouched tool	718	275	56	1	1050
Hammerstone	14	2	4	1	16
Flakes	2377	937	363	5	3682
Detached	591	404	327	1	1323
Fragment flake	3537	2246	698	5	6486
Chunks	804	607	273	5	1689
Total	8171	4522	1732	18	14443
Excavated m²	27	14	10	2	
Thickness (cm)	30	17	8	7	

analyses will allow us to provide a more precise correlation between the environmental conditions present during the different periods of occupation of Abric Pizarro with the evidence from glacial-interglacial cycles in the southeastern Pre-Pyrenees. Future analyses will aim to confirm the presence or absence of environmental proxies related of the last maximum ice extent (LMIE) identified in glaciofluvial and glacial deposits from the southeastern Pyrenees (e.g. Turu et al., 2023).

On the contrary, the anthracological data from units M, P and Q from Abric Pizarro is dominated by the presence of *Pinus sylvestris* type.

Differences between the palynological results, with a larger representation of evergreen oak and, anthracological data, dominated by pine, could be explained as reflecting this anthropogenic deliberate selection of specific wood (*Pinus*-type) for hearths. Nevertheless, both proxies provide different environmental resolution, with palynological data reflecting regional conditions compared to the local conditions represented by anthracological records.

Throughout MIS 3, *Pinus sylvestris* type is the most common taxa in anthracological records from the NE of Iberia (Allué et al., 2017a, 2017b, 2018). The occurrence of *Pinus sylvestris* type in the three layers from Abric Pizarro suggests a broader continuity of the environmental conditions into the MIS 3 represented at the nearby site of Cova Gran de Santa Linya (Allué et al., 2018). The recurrence of this taxa indicates the continuity of cold adapted forests that were developed in more or less humid or arid environments during the MIS 4. The lower temperatures during MIS 3 and MIS 4 allowed the spread of this mountain forest from the Pyrenees to the coastal areas in altitudes below their present distribution. In general, these forests were part of a mosaic-shaped landscape from which fuel was constantly available. According to most of the records, *Pinus sylvestris* type wood was the most available and therefore the most often used fuel to maintain fire (Vidal-Matutano et al., 2017; Allué et al., 2017a, 2017b, 2018).

Abric Pizarro constitutes further evidence of the importance of *Pinus sylvestris* type forests during periods of the Upper Pleistocene that were characterized by colder environmental conditions. Furthermore, the anthracological evidence from this site suggests the resilience of these forests throughout periods experiencing harsher conditions than today, as well as periods characterized by significant fluctuations in water availability associated with the transition between MIS 4 and MIS 3, as suggested by palynological (Burjachs et al., 2012) and small vertebrates (López-García et al., 2008; Laplana et al., 2016) data. Another line of evidence, the preliminary analysis of the zooarchaeological assemblage recovered in Abric Pizarro, provides significant data to interpret Neanderthal hunting practices diachronically during a period where scarce data is available. Due to the small excavated area in unit S, which has resulted in very few recovered remains, the fauna analysis from this unit is not considered further in the present study. Unit Q yielded a high percentage of *Capra pyrenaica*, small size ungulates and cervids, compared to the higher relative abundance of cervids and medium-size herbivores in units P and M. These trend contrast with the data from other MIS 4 Iberian sites. In northern Iberian sites, cervids dominate most of the assemblages, except for Arlampe, which is dominated by caprines (González et al., 2005; Demuro et al., 2023; Arceredillo et al., 2013; Rios-Garaizar et al., 2015; Lazuén and Altuna, 2012; Castaños, 2021). The higher caprine presence reported for the central plateau is not evident in Pizarro, although the percentage of small-sized herbivores remains stable (~20%) throughout the sequence. In Abric Pastor (Alcoi), the zooarchaeological results published from a discrete Neanderthal occupation (unit IVfH17) yielded a small amount of remains (78 bone fragments), identified to *Cervus elaphus* and *Capra pyrenaica* (Sossa-Ríos et al., 2022). Additional data from unit IVd (above unit IVfH17) based on around 200 bone fragments, indicate the presence of *Bos primigenius*, *Capra pyrenaica* and *Cervus elaphus*, with freshwater turtle (*Testudo hermanni*) yielding the greatest number of identified remains (NR = 129) (Connolly et al., 2019). In general, medium-size herbivores dominate these assemblages, followed by small-sized mammals.

These results suggest a similar taxonomic composition to that documented in units M and P from Abric Pizarro, which are dated to a similar chronology than these units at Abric Pastor (>63 ka). With a comparable orography and surrounding environment, with both shelters located in an enclosed ravine, the similarities observed between the assemblages from these two sites point towards Neanderthal groups adopting analogous subsistence strategies, where the immediate environment is successfully exploited through a range of diversified species and habitats.
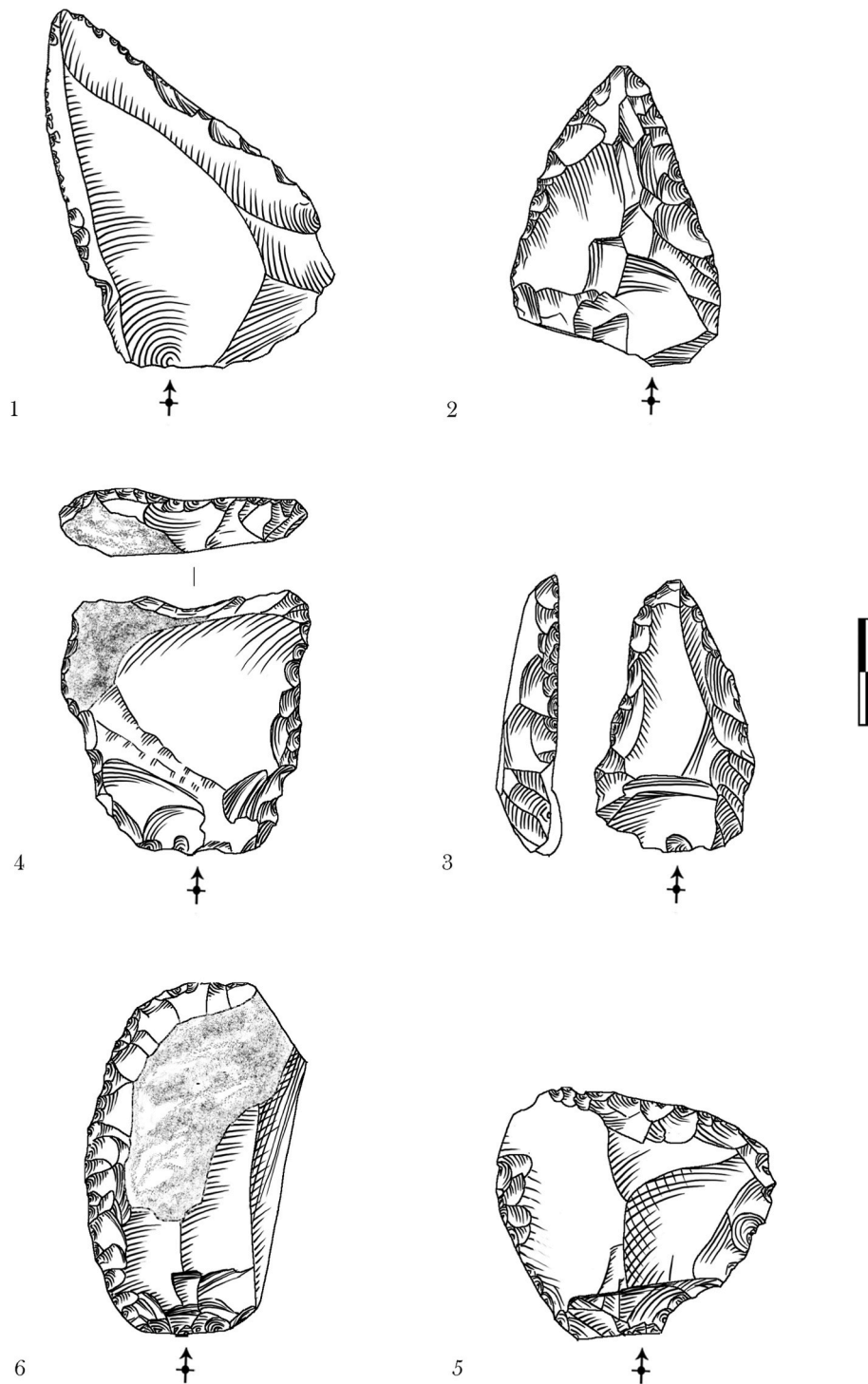
Fig. 9. Retouched tools documented in archaeological unit M. 1–3: Simple points; 4: Side scrapper with abrupt retouch; 5–6: Transversal side scrappers.

Due to the lack of zooarchaeological assemblages precisely dated to the MIS 4 in Northeast Iberia, as well as other factors related to deposits' integrity, it is complicated to compare the results obtained from Abric Pizarro to those published from some nearby sites. Gabasa cave (Huesca) has been characterised as a palimpsest, where accumulation generated by carnivores (i.e. hyenas) and Neanderthals are mingled. Additionally, problems with chronostratigraphic correlations hamper gathering data to interpret Neanderthal subsistence practices in this site (e.g. Utrilla et al., 2010). The assemblages from Gabasa (units a-h) are dominated by *Capra pyrenaica*, followed by *Cervus elaphus* and *Equus ferus* (Utrilla

et al., 2010). Nevertheless, the predominance of ibex in these assemblages is likely to result from carnivores (i.e. hyenas) actions.

The extensive research completed in sites like Abric Romaní, with systematic taphonomic data obtained from units I-M (ca. 47–54 ka) provide a remarkable framework to investigate Neanderthal lifeways during the MIS 3 in NE Iberia (e.g. Rosell et al., 2012; Marín et al., 2017; 2019). Although chronologically more recent than the archaeological units documented in Abric Pizarro, the taxonomic representation identified in Abric Romaní present similarities with Pizarro. Red deer and horse are present in every unit analysed from Abric Romani,

accompanied by large-sized herbivores (*Bos primigenius* and *Stephanorhinus hemitoechus*). Nevertheless, the low number of small-sized herbivores and caprines observed in Abric Romani contrast with their relative abundance in the lower unit of Abric Pizarro (Q), and a relatively stable presence throughout the sequence.

The zooarchaeological data from Cova Gran de Santa Linya, less than 10 km away from Abric Pizarro and with Neanderthal occupations dated to the MIS 3 (units S1E-S1B, 43-45ka), differs slightly from the data from Abric Pizarro. The Middle Palaeolithic zooarchaeological assemblages from Cova Gran are dominated by *Equus ferus*, followed by *Cervus elaphus*, with few remains (NISP) assigned to *Bos/Bison* sp. and *Capra pyrenaica*, although the differences in relative abundance of species becomes less significant when considering MNI values instead of NISP (Samper Carro 2015; Samper Carro et al., 2020). For the remains identified to size class, medium and large-sized herbivores yielded greatest number of bone fragments than small-sized mammals, although the latter represent at least 20% of the bone fragments assigned to size categories throughout the Middle Palaeolithic. Interestingly, the relative abundance of *Capra pyrenaica* and small-sized herbivores dramatically increases in unit 497D, dated to ca. 40ka and comprising the earliest Anatomically Modern Human (AMH) occupation documented in Cova Gran. These differences in the relative abundance of taxa between Neanderthal and AMH occupations are difficult to correlate which changes in environmental conditions, as discussed below, but might reflect differences in hunting strategies and the associated technological complexes (Mora et al., 2018; Samper Carro et al., 2020).

Large mammals are relatively resilient to environmental changes, and therefore drawing palaeoecological inferences from changes in their relative abundance is problematic. Nevertheless, the species represented in Abric Pizarro indicate a mosaic landscape in the proximity of the site. This would include heathlands, the preferential habitats for caprines and *Bos/Bison* sp., as well as forest and mixed woodlands which would have been exploited by Neanderthal groups.

Furthermore, the absence of turtles in the lower units could support the hypothesis of wetter conditions in the late-mid MIS 4 (c.68–59 ka) sequence in Abric Pizarro. Remains of pond turtles are relatively abundant in unit M and P, probably captured during times when the water surge at the bottom of Barranc de les Coves was active. Pond turtles are also recorded in the nearby site of Roca dels Bous, located by a river. Their absence in the lower units of Abric Pizarro could correlate with seasonal occupations during dry periods or the presence of periods of climatic instability during the mid-early MIS 4, with water fluctuations leading to drying of the water surge and related effects on turtle populations in the cave surroundings or seasonal occupations.

However, the elevated percentage of thermophilic taxa (evergreen *Quercus, Olea* and *Phillyrea*) and *Pinus*-type throughout the Abric Pizarro sequence suggests a generally stable climate, which might indicate that the changes in the prey composition and taxonomic representation could be related to human decisions. Anthropogenic modifications support interpretations of high efficiency in Neanderthal hunting of mammals of a different size range. As such, the Abric Pizarro assemblage indicates Neanderthals ability to exploit the local landscape. In this sense, further analysis of the faunal assemblage, including the characterisation of skeletal profiles and other derived quantitative units (i.e. MNI, MAU), will investigate whether the differences in the fauna could be linked to occupation function and seasonality (Westbury et al., 2024).

Another factor to consider regarding site function and seasonality resides in the significant differences observed among archaeological units and the techno-economic lithic categories identified, which may be related with the extent of the excavated surface and sedimentation rates. As such, changes in the lithic material density among units is unlikely to result from organisation choices related to settlement type and duration. Based on archaeological unit thickness, units M and P comprise low resolution palimpsests, or accumulations created by an uncertain number of events over a long temporal scale. On the contrary, units Q and S show medium/high resolution accumulations resulting from faster sedimentary rates, which represent more accurate occupation events to characterize Neanderthal behaviour (Fig. 2).

The lithic assemblage in unit M (centred on late MIS 4 and potentially spanning the MIS 4/3 transition) has been characterized as dominated by alike morphological Levallois tools, with simple and abrupt retouch side scrapers and points. In the lower units P and Q, which were most likely formed in the first half of MIS 4 and potentially span the MIS 5/4 transition, the knapping methods are characterized by the adoption of a Bifacial Centripetal Hierarchical (BCH) method associated with denticulated with simple and abrupt retouch. This trend contrast with those documented in nearby sites, where BCH methods are identified in MIS 3 occupations, and are commonly associated with notches and denticulates with continuous retouch.

These changes do not seem to correspond with temporal or cognitive aspects. At the same time, they highlight the important role played by factors such as site function, which would have been considered by Neanderthals when applying cognitive and technical behaviour likely to be related to specific circumstances and activities. These attributes, related to knapping methods variability, underscore how difficult it is to identify internal (chronocultural) or external (palaeoenvironmental) factors when interpreting techno-economic system variability during the Middle Palaeolithic. Likewise, it highlights the adaptability shown by Neanderthals in their techno-economic behaviours, which were anchored in cultural traditions spanning broad space-temporal extents (de la Torre et al., 2013, Casanova i Martí et al., 2014).

5. Conclusions

The preliminary results from Abric Pizarro improve our understanding of the Neanderthal populations' health before their disappearance, as well as contributing to discussions about the role of the Iberian Peninsula as a refugium during cold climatic periods.

The new chronometric ages support a late to early MIS 4 dating for the occupations documented in Abric Pizarro, increasing the number of sites identified from this period. Furthermore, the exploratory palynological and anthracological results presented contribute to characterizing environmental conditions during this glacial stage, suggesting that the southeastern Pre-Pyrenees might have been subjected to milder conditions than more septentrional latitudes, although experiencing sporadic climatic instability events. In general, palaeoenvironmental data suggest a vegetation change compared to current conditions, with the presence of montane pine and mediterranean patchy landscapes from the MIS 4 onwards. These results contribute to discussion regarding the presence of refugia in south Western Europe, which later could have contributed to an extended presence of Neanderthals in these areas.

The preliminary results from Abric Pizarro suggest that Neanderthal groups were adept hunters, with a broad knowledge of the surrounding landscape, which they exploited efficiently, as demonstrated in MIS 3 sites documented in the NE of the Iberian Peninsula (e.g. Abric Romani, L'Arbreda) and in Southwestern France (e.g. Les Pradelles, Chez-Pinaud, Mauran (Rendu). Our results demonstrate the value of opening new research lines at Abric Pizarro to better characterize the technical and cultural responses of Neanderthals in the southeast Pre-Pyrenees during the MIS 4, in order to complement the extensive data available from MIS 3 sites.

Future studies will characterize the Neanderthal occupations documented in Abric Pizarro in more detail. As such, the taphonomic analysis of the most recent zooarchaeological assemblages recently published (Westbury et al., 2024), as well as future analysis focused on the remaining zooarchaeological remains (including small prey), and the identification of lithic raw material and artefacts' horizontal spatial distribution will contribute significantly to increase our knowledge of the MIS 4 Neanderthal occupations in Western Europe.

CRediT authorship contribution statement

Sofia C. Samper Carro: Writing – original draft, Project administration, Methodology, Investigation, Funding acquisition, Formal analysis, Data curation, Conceptualization. **Susana Vega Bolivar:** Writing – review & editing, Project administration, Investigation, Data curation. **Jezabel Pizarro Barbera:** Writing – review & editing, Resources, Investigation. **Eboni Westbury:** Writing – review & editing, Investigation, Formal analysis. **Simon Connor:** Writing – review & editing, Methodology. **Ethel Allué:** Writing – review & editing, Methodology, Investigation. **Alfonso Benito-Calvo:** Writing – review & editing, Investigation. **Lee J. Arnold:** Writing – review & editing, Methodology. **Martina Demuro:** Writing – review & editing, Methodology, Formal analysis. **Gilbert J. Price:** Writing – review & editing, Methodology, Formal analysis. **Jorge Martinez-Moreno:** Writing – review & editing, Resources, Project administration. **Rafael Mora:** Writing – review & editing, Resources, Project administration, Investigation, Funding acquisition.

Declaration of competing interest

The authors declare that they have no known competing financial interests or personal relationships that could have appeared to influence the work reported in this paper.

Acknowledgments

Appendix A. Supplementary data

Supplementary data to this article can be found online at https://doi.org/10.1016/j.jas.2024.106038.

References

Agustí, J., Rubio-Campillo, X., 2017. Were Neanderthals responsible for their own extinction? Quat. Int. 431, 232–237.

Allué, E., Picornell-Gelabert, L., Daura, J., Sanz, M., 2017a. Reconstruction of the palaeoenvironment and anthropogenic activity from the upper Pleistocene/Holocene anthracological records of the NE Iberian Peninsula (Barcelona, Spain). Quat. Int. 457, 172–189.

Allué, E., Solé, A., Burguet-Coca, A., 2017b. Fuel exploitation among Neanderthals based on the anthracological record from Abric Romaní (Capellades, NE Spain). Quat. Int. 431, 6–15.

Allué, E., Martínez-Moreno, J., Roy, M., Benito-Calvo, A., Mora, R., 2018. Montane pine forests in NE Iberia during MIS 3 and MIS 2. A study based on new anthracological evidence from Cova gran (Santa Linya, Iberian pre-Pyrenees). Rev. Palaeobot. Palynol. 258, 62–72.

Arceredillo, D., Díez, C., 2009. Age of death and seasonality based on ungulate tooth remains from the Upper Pleistocene site of Valdegoba Burgos, Spain. Journal of Taphonomy 7, 73–89.

Arceredillo, D., Gómez-Olivencia, A., San Pedro-Calleja, Z., 2013. La fauna de macromamíferos de los niveles pleistocenos de la cueva de Arlanpe (Lemoa, Bizkaia). Kobie 3, 123–160.

Arnold, L.J., Roberts, R.G., 2009. Stochastic modelling of multi-grain equivalent dose (D_e) distributions: implications for OSL dating of sediment mixtures. Quat. Geochronol. 4, 204–230.

Arnold, L.J., Roberts, R.G., 2011. Paper I - optically stimulated luminescence (OSL) dating of perennially frozen deposits in north-central Siberia: OSL characteristics of quartz grains and methodological considerations regarding their suitability for dating. Boreas 40, 389–416.

Arnold, L.J., Roberts, R.G., Macphee, R.D.E., Willerslev, E., Tikhonov, A.N., Brock, F., 2008. Optical dating of perennially frozen deposits associated with preserved ancient plant and animal DNA in north-central Siberia. Quat. Geochronol. 3, 114–136.

Arnold, L.J., Roberts, R.G., Galbraith, R.F., DeLong, S.B., 2009. A revised burial dose estimation procedure for optical dating of young and modern-age sediments. Quat. Geochronol. 4, 306–325.

Arnold, L.J., Roberts, R.G., Macphee, R.D.E., Haile, J.S., Brock, F., Möller, P., Froese, D. G., Tikhonov, A.N., Chivas, A.R., Gilbert, M.T.P., Willerslev, E., 2011. Paper II - dirt, dates and DNA: OSL and radiocarbon chronologies of perennially frozen sediments in Siberia, and their implications for sedimentary ancient DNA studies. Boreas 40, 417–445.

Arnold, L.J., Demuro, M., Ruiz, M.N., 2012a. Empirical insights into multi-grain averaging effects from 'pseudo' single-grain OSL measurements. Radiat. Meas. 47, 652–658.

Arnold, L.J., Duval, M., Falguères, C., Bahain, J.J., Demuro, M., 2012b. Portable gamma spectrometry with cerium-doped lanthanum bromide scintillators: suitability assessments for luminescence and electron spin resonance dating applications. Radiat. Meas. 47, 6–18.

Arnold, L.J., Demuro, M., Navazo, M., Benito-Calvo, A., Pérez-González, A., 2013. OSL dating of the Middle Palaeolithic Hotel California site, Sierra de Atapuerca, north-central Spain. Boreas 42, 285–305.

Arnold, L.J., Demuro, M., Parés, J.M., Arsuaga, J.L., Aranburu, A., Bermúdez de Castro, J.M., Carbonell, E., 2014. Luminescence dating and palaeomagnetic age constraint on hominins from Sima de los Huesos, Atapuerca, Spain. J. Hum. Evol. 67, 85–107.

Arnold, L.J., Duval, M., Demuro, M., Spooner, N.A., Santonja, M., Pérez-González, A., 2016. OSL dating of individual quartz 'supergrains' from the Ancient Middle Palaeolithic site of Cuesta de la Bajada, Spain. Quat. Geochronol. 36, 78–101.

Arnold, L.J., Demuro, M., Spooner, N.A., Prideaux, G.J., McDowell, M.C., Camens, A.B., Reed, E.H., Parés, J.M., Arsuaga, J.L., Bermúdez de Castro, J.M., Carbonell, E., 2019. Single-grain TT-OSL bleaching characteristics: insights from modern analogues and OSL dating comparisons. Quat. Geochronol. 49, 45–51.

Arnold, L.J., Demuro, M., Power, R., Priya, Duval, M., Guilarte, V., Weij, R., Woodhead, J., White, L., Bourne, S., Reed, E.H., 2022. Examining sediment infill dynamics at Naracoorte Cave megafauna sites using multiple luminescence dating signals. Quat. Geochronol. 70, 101301.

Audouze, F., Karlin, C., 2017. La chaîne opératoire a 70 ans : qu'en ont fait les préhistoriens français. Journal of Lithic Studies 4, 1–69. https://doi.org/10.2218/jls.v4i2.2539.

Audouze, F., Bodu, P., Karlin, C., Julien, M., Pelegrin, J., Perlès, C., 2017. Leroi-Gourhan and the chaîne opératoire: a response to Delage. World Archaeol. 49 (5), 718–723.

Bailey, S.E., Lynch, J.M., 2005. Diagnostic differences in mandibular P4 shape between Neanderthals and anatomically modern humans. Am. J. Phys. Anthropol. 126, 268–277.

Banks, W.E., d'Errico, F., Peterson, A.T., Kageyama, M., Sima, A., Sánchez-Goñi, M.F., 2008. Neanderthal extinction by competitive exclusion. PLoS One 3, e3972.

Banks, W.E., Moncel, M.-H., Raynal, J.-P., Cobos, M.E., Romero-Alvarez, D., Woillez, M.-N., Faivre, J.-P., Gravina, B., d'Errico, F., Locht, J.-L., Santos, F., 2021. An ecological niche shift for Neanderthal populations in Western Europe 70,000 years ago. Sci. Rep. 11, 5346. https://doi.org/10.1038/s41598-021-84805-6.

Behrensmeyer, A.K., 1978. Taphonomic and ecologic information from bone weathering. Paleobiology 4, 150–162.

Blanco, E., Casado, M.A., Costa, M., Escribano, R., García, M., Génova, M., et al., 1998. *Los bosques Ibéricos: Una Interpretación Geobotánica*. 1998. Geoplaneta.

Blumenschine, R.J., Marean, C.W., Capaldo, S.D., 1996. Blind-test of inter-analysts correspondence and accuracy in the identification of cut marks, percussion marks, and carnivore tooth marks on bone surfaces. J. Archaeol. Sci. 23, 493–507.

Bocherens, H., Drucker, D.G., 2006. Dietary competition between Neanderthals and modern humans: insights from stable isotopes. In: Conard, N.J. (Ed.), *When Neanderthals and Modern Humans Met*. Tübingen Publications in Prehistory, pp. 129–143.

Boëda, E., 1990. De la surface au volume analyse des conceptions des débitages levallois et laminaire. Memories Musee de Prehistorie d'Ille-de-France 3, 63–67.

Boëda, E., 1993. Le débitage discoïde et le débitage levallois récurrent centripète. Bull. Soc. Prehist. Fr. 90, 392–404.

Boëda, E., 2005. Techno-logique & Technologie. Une Paléo-histoire des objets lithiques tranchants. Archéo-éditions.

Boëda, E., Geneste, J.M., y Meignen, L., 1990. Identification de chaînes opératoires lithiques du Paleolithique Ancien et Moyen. Paléo 2, 43–80.

Bøtter-Jensen, L., Mejdahl, V., 1988. Assessment of beta dose-rate using a GM multicounter system. Int. J. Radiat. Appl. Instrum. Part A 14, 187–191.

Bowler, J.M., Johnston, H., Olley, J.M., Prescott, J.R., Roberts, R.G., Shawcross, W., Spooner, N.A., 2003. New ages for human occupation and climatic change at Lake Mungo, Australia. Nature 421, 837–840.

Brennan, B.J., 2003. Beta doses to spherical grains. Radiat. Meas. 37, 299–303.

Burjachs, F., López-García, J.M., Allué, E., Blain, H.A., Rivals, F., Bennàsar, M., Expósito, I., 2012. Palaeoecology of Neanderthals during Dansgaard–Oeschger cycles in northeastern Iberia (abric Romaní): from regional to global scale. Quaternaty International 247, 26–37.

Bustos-Pérez, G., Baena, J., Vaquero, M., 2023. What lies in between: levallois, discoid and intermediate methods. Journal of Lithic Studies 10 (2), 32. https://doi.org/10.2218/jls.7132.

Camuera, J., Jiménez-Moreno, G., Ramos-Román, M.J., García-Alix, A., Toney, J.L., Anderson, R.S., Jiménez-Espejo, F., Bright, J., Webster, C., Yanes, Y., Carrión, J.S., 2019. Vegetation and climate changes during the last two glacial-interglacial cycles in the western Mediterranean: a new long pollen record from Padul (southern Iberian Peninsula). Quat. Sci. Rev. 205, 86–105. https://doi.org/10.1016/j.quascirev.2018.12.013.

Capaldo, S.D., Blumenschine, R.J., 1994. A quantitative diagnosis of notches made by hammerstone percussion and carnivore gnawing on bovid long bones. Am. Antiq. 59, 724–748.

Casanova, J., Martínez Moreno, J., Mora, R., De la Torre, I., 2009. Stratégies techniques dans la Paléolithique Moyen du sud-est des Pyrénées. L'Anthropologie 113, 313–340.

Casanova i Martí, J., Roda Gilabert, X., Martínez-Moreno, J., Mora, R., 2014. Débitage, façonnage et diversité des systèmes techniques du Moustérien à Tragó (Pré-Pyrénées de Lleida, Catalogne. In: Jaubert, J., Fourment, N., Depaepe, P. (Eds.), *Transitions, ruptures et continuité en Préhistoire* Vol. 2 Paléolithique et Mésolithique. Société Préhistorique Française, Paris, pp. 139–154.

Castaños, P., 2021. Estudio de la fauna de macromamíferos del yacimiento del Pleistoceno Superior de la cueva de Covalejos. In: Montes Barquín, R., Sanguino González, J. (Eds.), La Cueva de Covalejos (Velo de Piélagos, Cantabria). Museo de Prehistoria y Arqueología de Cantabria, pp. 106–125.

Castaños, P., Guenaga, A., López-Quintana, J.C., 2004. Cueva de Atxahakoa (Forua) III Campaña de excavaciones. Arkeoikuska Investig. Arqueol, pp. 327–329.

Cheng, H., Edwards, R.L., Hoff, J., Gallup, C.D., Richards, D.A., Asmerom, Y., 2000. The half-lives of uranium-234 and thorium-230. Chem. Geol. 169 (1–2), 17–33.

Churchill, S.E., 2014. Thin on the Ground: Neanderthal Biology, Archaeology and Ecology. Wiley-Blackwell.

Connolly, R., Jambrina-Enríquez, M., Herrera-Herrera, A.V., Vidal-Matutano, P., Fagoaga, A., Marquina-Blasco, R., Marin-Monfort, M.D., Ruiz-Sanchez, F.J., Laplana, C., Bailon, S., Perez, L., Leierer, L., Hernandez, C.M., Galvan, B., Mallol, C., 2019. A multiproxy record of palaeoenvironmental conditions at the Middle Palaeolithic site of Abric del Pastor (Eastern Iberia). Quat. Sci. Rev. 225, 106023.

Daura, J., Sanz, M., Demuro, M., Arnold, L.J., Costa, A., Moreno, J., Freitas, C., Lopes, V., Éguez, N., Hoffman, D., Benson, A., Cabanes, D., García-Targa, J., Fullola, J.M., 2021. A new chronological framework and site formation history for Cova del Gegant (Barcelona): Implications for Neanderthal and Anatomically Modern Human occupation of NE Iberian Peninsula. Quat. Sci. Rev. 270, 107141.

de la Torre, I., Martínez Moreno, J., Mora, R., 2012. When bones are not enough: lithic refits and occupation dynamics in the Middle Palaeolithic Level 10 of Roca dels Bous (Catalonia, Spain). In: Seetah, K., Gravina, B. (Eds.), Bones for Tools-Tools for Bones. The Interplay between Objects and Objectives. McDonald Institute for Archaeological Research, pp. 13–23.

de la Torre, I., Martínez-Moreno, J., Mora, R., 2013. Change and Stasis in the Iberian middle Paleolithic: considerations on the significance of Mousterian technological variability. Curr. Anthropol. 54 (S8), S320–S336.

Demuro, M., Arnold, L.J., Froese, D.G., Roberts, R.G., 2013. OSL dating of loess deposits bracketing Sheep Creek tephra beds, northwest Canada: dim and problematic single-grain OSL characteristics and their effect on multi-grain age estimates. Quat. Geochronol. 15, 67–87.

Demuro, M., Arnold, L.J., Aranburu, A., Gómez-Olivencia, A., Arsuaga, J.L., 2019. Single-grain OSL dating of the Middle Palaeolithic site of Galería de las Estatuas, Atapuerca (Burgos, Spain). Quat. Geochronol. 49, 254–261.

Demuro, M., Arnold, L.J., González-Urquijo, J., Lazuen, T., Frochoso, M., 2023. Chronological constraint of Neanderthal cultural and environmental changes in southwestern Europe. MIS 5–MIS 3 dating of the Axlor site (Biscay, Spain). J. Quat. Sci. 38, 890–920.

Díez, J.C., 2007. Huellas de descarnado en el Paleolítico Medio: La cueva de Valdegoba Burgos. Zona Arqueol 7, 304–317.

Duval, M., Arnold, L.J., 2013. Field gamma dose-rate assessment in natural sedimentary contexts using LaBr₃(Ce) and NaI(Tl) probes: a comparison between the "threshold" and "windows" techniques. Appl. Radiat. Isot. 74, 36–45.

d'Errico, F., Sánchez-Goñi, M.F., 2003. Neanderthal extinction and the Millenian scale climatic variability of OIS 3. Quat. Sci. Rev. 22, 769–788.

Euba, L., 2008. Análisis antracológico de estructuras altimontanas en el valle de la Vansa Sierra del Cadí (Alt Urgell) y en el valle del Madriu (Andorra): explotación de recursos forestales del Neolítico medio a época moderna. PhD Thesis, Universitat Rovira i Virgili.

Falguères, C., Yokoyama, Y., Arrizabalaga, A., 2005. La geocronología del yacimiento pleistocénico de Lezetxiki (Arrasate, País Vasco). Crítica de las dataciones existentes y algunas nuevas aportaciones. Munibe 57, 93–106.

Fernandez-Jalvo, Y., Andrews, P., 2016. Atlas of taphonomic identifications: 1001+ images of fossil and recent mammal bone modification. Vertebrate Paleobiology and Paleoanthropology. Springer Netherlands, Dordrecht. https://doi.org/10.1007/978-94-017-7432-1.

Fisher, J.W., 1995. Bone surface modifications in zooarchaeology. J. Archaeol. Method Theor 2, 7–68.

Folch, R., Natural, I.C.D.H., 1986. La Vegetació Dels Països Catalans. Ketres. Institut d'Estudis Catalans.

Galbraith, R.F., Roberts, R.G., Laslett, G.M., Yoshida, H., Olley, J.M., 1999. Optical dating of single and multiple grains of quartz from Jinmium rock shelter, northern Australia: Part I, experimental design and statistical models. Archaeometry 41, 339–364.

Galbraith, R.F., Roberts, R.G., Yoshida, H., 2005. Error variation in OSL palaeodose estimates from single aliquots of quartz: a factorial experiment. Radiat. Meas. 39, 289–307.

García-Ruiz, J.M., Martí-Bono, C., Peña-Monné, J.L., Sancho, C., Rhodes, E.J., Valero-Garcés, B., González-Sampériz, P., Moreno, A., 2013. Glacial and fluvial deposits in the Aragón valley, central-western Pyrenees: chronology of the Pyrenean late Pleistocene glaciers. Geogr. Ann. Phys. Geogr. 95, 15–32.

Geneste, J.-M., 1991. Systhèmes techniques de production lithique:Variations techno-économiques dans les processus de réalisation des outillages paléolithiques. Tech. Cult. 17–18, 1–35.

González, J., Ibañez, J.J., Ríos, J., Bourguignon, L., Castaños, P., Tarriño, A., 2005. Excavaciones recientes en Axlor. Movilidad y planificación de actividades en grupos de neandertales. Mus. Altamira Monogr. 20, 527–539.

Gonzalez, A.R., García-Tabernero, A., Morales, J.I., 2023. Filogeografía de los Neandertales de la península Ibérica. Estado de la cuestión. Cuaternario Geomorfol. 37 (3–4), 9–20.

González-Sampériz, P., Gil-Romera, G., García-Prieto, E., Aranbarri, J., Moreno, A., Morellón, M., Sevilla-Callejo, M., Leunda, M., Santos, L., Franco-Múgica, F., Andrade, A., Carrión, J.S., Valero-Garcés, B.L., 2020. Strong continentality and effective moisture drove unforeseen vegetation dynamics since the last interglacial at inland Mediterranean areas: the Villarquemado sequence in NE Iberia. Quat. Sci. Rev. 242, 106425 https://doi.org/10.1016/j.quascirev.2020.106425.

Grün, R., McDermott, F., 1994. Open system modelling for U-series and ESR dating of teeth. Quat. Sci. Rev. 13 (2), 121–125.

Guérin, G., Mercier, M., Adamiec, G., 2011. Dose-rate conversion factors: update. Ancient TL 29, 5–8.

Helmens, K.F., 2014. The Last Interglacial–Glacial cycle (MIS 5–2) re-examined based on long proxy records from central and northern Europe. Quat. Sci. Rev. 86, 115–143. https://doi.org/10.1016/j.quascirev.2013.12.012.

Hocknull, S.A., Lewis, R., Arnold, L.J., Pietsch, T., Joannes-Boyau, R., Price, G.J., Moss, P., Wood, R., Dosseto, A., Louys, J., Olley, J., Lawrence, R.A., 2020. Extinction of eastern Sahul megafauna coincides with sustained environmental deterioration. Nat. Commun. 11, 2250.

Jacobs, Z., Duller, G.A.T., Wintle, A.G., 2006a. Interpretation of single-grain Dₑ distributions and calculation of Dₑ. Radiat. Meas. 41, 264–277.

Jacobs, Z., Duller, G.A.T., Wintle, A.G., Henshilwood, C.S., 2006b. Extending the chronology of deposits at Blombos Cave, South Africa, back to 140 ka using optical dating of single and multiple grains of quartz. J. Hum. Evol. 51, 255–273.

Laplace, G., 1972. La typologie analytique et structurale: Base rationnelle d'étude des industries lithiques et osseuses. CNRS, Marsella.

Laplace, G., Saénz de Buruaga, A. 2002-2003. Typologie analytique et structurale des complexes du Moustérien de la Grotte Gatzarria (Ossas-Suhare, Pays Basque) et de leurs relations avec ceuz de l'Abri Olha 2 (Cambo, Pays Basque). Pyrenae 33–34: 81-163.

Laplana, C., Sevilla, P., Blain, H.A., Arriaza, M.C., Arsuaga, J.L., Pérez-González, A., Baquedano, E., 2016. Cold-climate rodent indicators for the Late Pleistocene of central Iberia: New data from the Buena Pinta Cave (Pinilla del Valle, Madrid region, Spain). Comptes Rendus Palevol 15 (6), 696–706.

Lazuén, T., Altuna, J., 2012. Organización tecnológica de las primeras sociedades neandertales del Cantábrico. Lectura de las industrias líticas y de la fauna de los niveles inferiores (V, VI y VII) de la cueva de Lezetxiki. Zephyrvs 69, 41–74.

Lemonnier, P., 1983. L'etude des systemes techniques, une urgence en technologie culturelle. Technologie culturelle 1, 11–34.

Lemonnier, P., 1993. Technological Choices. Routledge, Londres/Nueva York.

Lemonnier, P., 2010. Retour sur "L'Étude des systèmes techniques". Tech. Cult. 54–55 (2), 46–48.

Lewis, C., McDonald, E., Sancho, C., Peña, J.L., Rhodes, E., 2009. Climatic implications of correlated Upper Pleistocene glacial and fluvial deposits on the Cinca and Gállego Rivers, NE Spain. Global Planet. Change 67, 141–152.

Lewis, R., Tibby, J., Arnold, L.J., Barr, C., Marshall, J., McGregor, G., Gadd, P., Yokoyama, Y., 2020. Insights into subtropical Australian aridity from Welsby Lagoon, north Stradbroke Island, over the past 80,000 years. Quat. Sci. Rev. 234, 106262.

Lisiecki, L.E., Raymo, M.E., 2005. A Pliocene-Pleistocene stack of 57 globally distributed benthic δ 18O records. Paleoceanography 20, 1–17.

López-García, J.M., Blain, H.A., Cuenca-Bescos, G., Arsuaga, J.L., 2008. Chronological, environmental, and climatic precisions on the Neanderthal site of the Cova del Gegant (Sitges, Barcelona, Spain). J. Hum. Evol. 55 (6), 1151–1155.

Ludwig, K.R., 2003. Users Manual for Isoplot/Ex Version 3.0: A Geochronological Toolkit for Microsoft Excel. Berkeley Geochronology Centre, Berkeley.

Ludwig, K.R., Simmons, K.R., Szabo, B.J., Winograd, I.J., Landwehr, J.M., Riggs, A.C., Hoffman, R.J., 1992. Mass-spectrometric 230Th-234U-238-U dating of the Devils Hole calcite vein. Science 258, 284–287.

Marín, J., Saladié, P., Rodríguez-Hidalgo, A., Carbonell, E., 2017. Ungulate carcass transport strategies at the middle palaeolithic site of abric Romaní (Capellades, Spain). Comptes Rendus Palevol 16 (1), 103–121.

Marín, J., Rodríguez-Hidalgo, A., Vallverdú, J., Gómez de Soler, B., Rivals, F., Rabuñal, J. R., Pineda, A., Chacón, M.G., Carbonell, E., Saladié, P., 2019. Neanderthal logistic

mobility during MIS 3: Zoarchaeological perspective of abric Romaní level P (Spain). Quat. Sci. Rev. 225, 106033.

Martin, L., Mercier, N., Incerti, S., Lefrais, Y., Pecheyran, C., Guerin, G., Jarry, M., Bruxelles, L., Bon, F., Pallier, C., 2015. Dosimetric study of sediments at the beta dose rate scale: characterization and modelization with the DosiVox software. Radiat. Meas. 81, 134–141.

Martínez Moreno, J., Mora, R., De la Torre, I., 2010. The middle-to-upper palaeolithic transition in Cova gran (Catalunya, Spain) and the extinction of Neanderthals in the Iberian Peninsula. J. Hum. Evol. 58, 16.

Martínez-Moreno, J., González Marcén, P., Mora, R., 2011. Data matrix (DM) codes: a technological process for the management of the archaeological record. J. Cult. Herit. 12 (2), 134–139.

Martínez-Moreno, J., Mora Torcal, R., Roy Sunyer, M., Benito-Calvo, A., 2016. From site formation processes to human behaviour: towards a constructive approach to depict palimpsests in Roca dels Bous. Quat. Int. 417, 82–93.

Mejdahl, V., 1979. Thermoluminescence dating: beta-dose attenuation in quartz grains. Archaeometry 21, 61–72.

Mejdahl, V., 1987. Internal radioactivity in quartz and feldspar grains. Ancient TL 5, 10–17.

Menéndez, L., Rosell, J., Canals, A., Mosquera, M., 2009. El nivel G de las Fuentes de San Cristóbal (Huesca, España): nuevas aportaciones al estudio del Paleolítico medio en el Pre-Pirineo aragonés. Rev. C G 23, 95–111.

Mir, R., Salas, A., 2000. La cueva de la Fuente del Trucho y su industria lítica arcaizante del Pleniglacial superior (Colungo, Huesca). Bolskan 17, 9–32.

Montes, L., Utrilla, P., Martínez-Bea, M., 2006. Trabajos recientes en yacimientos musterienses de Aragón: una revisión de la transición Paleolítico Medio/Superior en el Valle del Ebro. In: Miscelania En Homenaje a Victoria Cabrera. Zona Arqueológica, pp. 215–232.

Montes, L., Domingo, R., Sampietro-Vattuone, M.M., Medialdea, A., Peña Monné, J.L., 2021. El yacimiento muesteriense de Roca San Miguel (Arén, Prepirineo de Huesca). Cuaternario Geomorfol. 35, 99–117. https://doi.org/10.17735/cyg.v35i1-2.89388.

Moore, P., Webb, J., Collinson, M., 1991. Pollen Analysis. Blackwell Scientific Publications, Oxford.

Mora, R., de la Torre Sáinz, I., Martínez-Moreno, J., 2010. ArqueoUAB: a systematic archaeographic approach for the analysis of Palaeolithic sites. In: Melero, F.J., Cano, P., Revelles, J (Eds.), Computer Applications and Quantitative Methods in Archaeology. Granada: CAA Fusion of Cultures, pp. 125–128.

Mora, R., Benito Calvo, A., Martínez Moreno, J., González Marcén, P., De la Torre, I., 2011. Chrono-stratigraphy of the upper Pleistocene and Holocene archaeological sequence in Cova gran (south-eastern pre-Pyrenees, Iberian Peninsula). J. Quat. Sci. 26, 10.

Mora, R., Martinez-Moreno, J., Roy Sunyer, M., Benito Calvo, A., Polo Díaz, A., Samper Carro, S.C., 2018. Contextual, technological and chronometric data from Cova Gran: their contribution to discussion of the Middle-to-Upper Paleolithic transition in northeastern Iberia. Quat. Int. 474, 30–43.

Mora, R., Roy Sunyer, M., Martínez-Moreno, J., Benito-Calvo, A., Samper Carro, S., 2020. Inside the palimpsest: identifying short occupations in the 497D level of Cova gran (Iberia). In: Cascalheira, J., Picin, A. (Eds.), *Short-Term Occupations in Paleolithic Archaeology*. Interdisciplinary Contributions to Archaeology. Springer, Cham. https://doi.org/10.1007/978-3-030-27403-0_3.

Nathan, R.P., Thomas, P.J., Jain, M., Murray, A.S., Rhodes, E.J., 2003. Environmental dose rate heterogeneity of beta radiation and its implications for luminescence dating: Monte Carlo modelling and experimental validation. Radiat. Meas. 37, 305–313.

Neeson, T.M., Van Rijn, I., Mandelik, Y., 2013. How taxonomic diversity, community structure, and sample size determine the reliability of higher taxon surrogates. Ecol. Appl. 23 (5), 1216–1225.

Nicholson, R.A., 1993. A morphological investigation of burnt animal bone and an evaluation of its utility in archaeology. J. Archaeol. Sci. 20, 411–428.

Ochando, J., Carrión, J.S., Blasco, R., Rivals, F., Rufà, A., Amorós, G., Munuera, M., Fernández, S., Rosell, J., 2020a. The Late Quaternary pollen sequence of Toll Cave, a palaeontological site with evidence of human activities in Northeastern Spain. Quat. Int. 554, 1–14.

Ochando, J., Carrión, J.S., Blasco, R., Rivals, F., Rufà, A., Demuro, M., Arnold, L.J., Amorós, G., Munuera, M., Fernández, S., Rosell, J., 2020b. Neanderthals in a highly diverse, Mediterranean-Eurosiberian forest ecotone: the Pleistocene pollen record of Teixoneres Cave, Northeastern Spain. Quat. Sci. Rev. 241, 106429.

Ochando, J., Amorós, G., Carrión, J.S., Fernández, S., Munuera, M., Camuera, J., Jiménez-Moreno, G., González-Sampériz, P., Burjachs, F., Marín-Arroyo, A.B., Roksandic, M., Finlayson, C., 2022. Iberian Neanderthals in forests and savannahs. J. Quat. Sci. 37, 335–362. https://doi.org/10.1002/jqs.3339.

Pante, M.C., Blumenschine, R.J., Capaldo, S.D., Scott, R.S., 2012. Validation of bone surface modification models for inferring fossil hominin and carnivore feeding interactions, with reapplication to FLK 22, Olduvai Gorge, Tanzania. J. Hum. Evol. 63, 395–407.

Pawley, S.M., Bailey, R.M., Rose, J., Moorlock, B.S.P., Hamblin, R.J.O., Booth, S.J., Lee, J.R., 2008. Age limits on Middle Pleistocene glacial sediments from OSL dating, north Norfolk, UK. Quat. Sci. Rev. 27, 1363–1377.

Peña, J.L., Sancho, C., Lewis, C., McDonald, E., Rhodes, E., 2004. Datos cronológicos de las morrenas terminales del glaciar del Gállego y su relación con las terrazas fluvioglaciares (Pirineo de Huesca). En. In: Peña Monné, J.L., Longares, L.A., Sánchez Fabre, Aladrén y M. (Eds.), Geografía Física de Aragón. Aspectos generales y.

Peña-Monné, J.L., Montes, L., Sampietro-Vattuone, M.M., Domingo, R., Medialdea, A., Bartolomé, M., Rubio Fernández, V., García Giménez, R., Turu, V., Ros, X., Baró, P., Bernal-Wormull, J.L., Edwards, R.L., 2021. The Mousterian site of Roca san Miguel

(Arén, Huesca, Spain). Geomorphological, chronological, and paleoenvironmental context from the penultimate to the last glacial cycle. Quat. Res. 1–20. https://doi.org/10.1017/qua.2021.61.

Pickering, T.R., 2002. Reconsideration of criteria for differentiating faunal assemblages accumulated by hyenas and hominids. Int. J. Osteoarchaeol. 12, 122–141.

Pickering, T.R., Egeland, C.P., 2006. Experimental patterns of hammerstone percussion damage on bones: implications for inferences of carcass processing by humans. J. Archaeol. Sci. 33, 459–469.

Pike, A.W.G., Hedges, R.E.M., 2002. U-series dating of bone using the diffusion-adsorption model. Geochem. Cosmochim. Acta 66 (24), 4273–4286.

Pizarro, J., Roy, M., Roda, X., Vega, S., Samper, S., Plasencia, J., Casanova, J., López, M., González Marcén, P., Martínez Moreno, J., Mora, R., 2013. Nous elements de reflexió al voltant del poblament del Prepirineu oriental al llarg del Plistocè superior i l'holocè. In: III Col.Loqui d'Arqueologia d'Odèn (Solsonès). Patronat del Museu Diocesà i Comarcal de Solsona, pp. 17–26.

Prescott, J.R., Hutton, J.T., 1994. Cosmic ray contributions to dose rates for luminescence and ESR dating: large depths and long-term time variations. Radiat. Meas. 23, 497–500.

Price, G.J., Feng, Y.X., Zhao, J.X., Webb, G.E., 2013. Direct U–Th dating of vertebrate fossils with minimum sampling destruction and application to museum specimens. Quat. Geochronol. 18, 1–8.

Price, G.J., Fitzsimmons, K.E., Nguyen, A.D., Zhao, J.X., Feng, Y.X., Sobbe, I.H., Godthelp, H., Archer, M., Hand, S.J., 2021. New ages of the world's largest-ever marsupial: Diprotodon optatum from Pleistocene Australia. Quat. Int. 603, 64–73.

Rees-Jones, J., 1995. Optical dating of young sediments using fine-grain quartz. Ancient TL 13, 9–14.

Rees-Jones, J., Tite, M.S., 1997. Optical dating results for British archaeological sediments. Archaeometry 39, 177–187.

Reille, M., 1992. *Pollen et Spores d'Europe et d'Afrique du Nord* (3 vols). Laboratoire de Botanique Historique et Palynologie, Marseille.

Revelles, J., Allué, E., Alcolea, M., Antolín, F., Berihuete-Azorín, M., Expósito, I., Garay, B., Mas, B., Piqué, R., Obea, L., Val-Peón, C., Burjachs, F., 2022. Site formation processes, human activities and palaeoenvironmental reconstructions from archaeobotanical records in cave and rock-shelter sites in NE Iberia. Rev. Palaeobot. Palynol. 299, 104612 https://doi.org/10.1016/j.revpalbo.2022.104612.

Rios-Garaizar, J., Garate Maidagan, D., Gómez-Olivencia, A., Iriarte, E., Arceredillo-Alonso, D., Iriarte-Chiapusso, M.J., Garcia-Ibaibarriaga, N., García-Moreno, A., Gutierrez-Zugasti, I., Torres, T., Aranburu, A., Arriolabengoa, M., Bailón, S., Murelaga, X., Ordiales, A., Ortiz, J.E., Rofes, J., San Pedro, J., 2015. Short-term Neandertal occupations in the late middle Pleistocene of Arlanpe (Lemoa, northern Iberian Peninsula). Comptes Rendus Palevol 14, 233–244. https://doi.org/10.1016/j.crpv.2014.11.006.

Roiron, P., Chabal, L., Figueiral, I., Terral, J.F., Ali, A.A., 2013. Palaeobiogeography of Pinus nigra Arn. subsp. salzmannii (Dunal) Franco in the north-western Mediterranean Basin: a review based on macroremains. Rev. Palaeobot. Palynol. 194, 1–11.

Romagnoli, F., Rivals, F., Benazzi, S. (Eds.), 2022. Updating Neanderthals: Understanding Behavioral Complexity in the Late Middle Paleolithic. Academic Press, Amsterdam.

Rosell, J., Huguet, R., Aimene, M., Angelucci, D.E., Canals, A., Pastó, I., Rodríguez, X., 2000. El yacimiento de las Fuentes de San Cristóbal (Veracruz, Huesca): un nuevo enclave del Paleolítico Medio en el Prepirineo. Presented at the Paleolítico da Península Ibérica. Actas do 3º Congresso de Arqueologia Peninsular II, 235–249.

Rosell, J., Cáceres, I., Blasco, R., Bennasar, M., Bravo, P., Campeny, G., Esteban-Nadal, M., Fernández'Laso, M.C., Gabucio, M.J., Huguet, R., Ibáñez, N., Martín, P., Rivals, F., Rodríguez-Hidalgo, A., Saladié, P., 2012. A zooarchaeological contribution to establish occupational patterns at Level J of Abric Romaní (Barcelona, Spain). Quat. Int. 247, 69–84.

Roy, M., 2015. Deconstructing archaeological palimpsests: applicability of GIS algorithms for the automated generation of cross sections. CAA2015 Keep the revolution going, Siena. Archaeopress Archaeology 407, 414.

Roy, M., Tarriño, A., Benito Calvo, A., Mora, R., Martínez Moreno, J., 2013. Aprovisionamiento de sílex en el Prepirineo Oriental: el nivel arqueológico 497C de Cova Gran (Santa Linya, Lleida). Trab. Prehist. 70 (1), 7–27.

Ruiz, M.N., Benito-Calvo, A., Alonso-Alcalde, R., Alonso, P., Fuente, H.D.L., Santamaría, M., Santamaría, C., Álvarez-Vena, A., Arnold, L.J., Iriarte-Chiapusso, M.J., Demuro, M., Lozano, M., Ortiz, J.E., Torres, T., 2021. Late Neanderthal subsistence strategies and cultural traditions in the northern Iberia Peninsula: insights from Prado Vargas, Burgos, Spain. Quat. Sci. Rev. 254, 106795.

Saladié, P., Huguet, R., Díez, C., Rodríguez-Hidalgo, A., Cáceres, I., Vallverdú, J., Rosell, J., Bermúdez De Castro, J.M., Carbonell, E., 2011. Carcass transport decisions in Homo antecessor subsistence strategies. J. Hum. Evol. 61, 425–446. https://doi.org/10.1016/j.jhevol.2011.05.012.

Sambridge, M., Grün, R., Eggins, S., 2012. U-series dating of bone in an open system: the diffusion-adsorption-decay model. Quat. Geochronol. 9, 42–53.

Samper Carro, S.C., 2015. Patrones de subsistencia durante el Paleolítico medio/superior en el Nordeste peninsular. Universitat Autonoma de Barcelona. PhD thesis. http://hdl.handle.net/10803/285739.

Samper Carro, S.C., Martínez-Moreno, J., Mora, R., 2020. Wind of change: zooarchaeological approach to the middle–upper palaeolithic transition in Cova gran of Santa Linya (Lleida, south-eastern pre-Pyrenees). J. Paleolit. Archaeol. 3, 989–1031.

Sánchez-Goñi, M.F., 2022. The climatic and environmental context of the Late Pleistocene. In: Romagnoli, F., Rivals, F., Benazzi, S. (Eds.), Updating Neanderthals. Understanding Behavioural Complexity in the Late Middle Paleolithic. Elsevier Academic Press, London, UK, pp. 17–38.

Sancho, C., Peña, J.L., Lewis, C., McDonald, E., Rhodes, E., 2003. Preliminary dating of glacial and fluvioglacial deposits in the Cinca River Valley (NE Spain): chronological evidence for the Glacial maximum in the Pyrenees? En. In: Ruiz Zapata, M.B., et al. (Eds.), Quaternary Climatic Changes and Environmental Crises in the Mediterranean Region. Univ., Alcalá de Henares-M° Ciencia y Tecnología-INQUA.

Sancho, C., Arenas, C., Pardo, G., Peña-Monné, J.L., Rhodes, E., Bartolomé, M., García-Ruiz, J.M., Martí-Bono, C., 2018. Glaciolacustrine deposits formed in an ice-dammed tributary valley in South-central Pyrenees: new evidence for the Late Pleistocene climate evolution. Sediment. Geol. 366, 47–66.

Santamaría, D., Montes, L., Utrilla, P., 2010. Variabilidad técnica del Paleolítico Medio en el Valle del Ebro: La Cueva de Moros I de Gabasa (Peralta de Calasanz, Huesca), vol. 14. D'Arqueologia, Treb.

Schweingruber, F.H., 1990. Anatomy of European Woods. *Anatomy of European Woods*.

Shipman, P., Foster, G., Schoeninger, M., 1984. Burnt bones and teeth: an experimental study of color, morphology, crystal structure and shrinkage. J. Archaeol. Sci. 11, 307–325.

Smedley, R.K., Duller, G.A.T., Rufer, D., Utley, J.E.P., 2020. Empirical assessment of beta dose heterogeneity in sediments: implications for luminescence dating. Quat. Geochronol. 56, 101052.

Sossa-Ríos, S., Mayor, A., Hernández, C.M., Bencomo, M., Pérez, L., Galván, B., Mallol, C., Vaquero, M., 2022. Multidisciplinary evidence of an isolated Neanderthal occupation in Abric del Pastor (Alcoi, Iberian Peninsula). Sci. Rep. 12, 15883.

Stewart, J.R., 2005. The ecology and adaptation of Neanderthals during the non-analogue environment of Oxygen Isotope Stage 3. Quat. Int. 137, 35–46.

Stiner, M.C., Kuhn, S.L., Weiner, S., Bar-Yosef, O., 1995. Differential burning, recrystallization and fragmentation of archaeological bone. J. Archaeol. Sci. 22, 223–237.

Turu, V., Peña-Monné, J.L., Cunha, P.P., Jalut, G., Buylaert, J.-P., Murray, A.S., Bridgland, D., Faurschou-Knudsen, M., Oliva, M., Carrasco, R., Ros, X., Turu-Font, L., Ventura-Roca, J., 2023. Glacial-interglacial cycles in south-eastern Pyrenees since ~180 ka: the dated records of the Upper Segre River and main tributaries (NE Spain-Andorra-SE France). Quat. Res. 1–28.

Utrilla, P., Montes, L., Blasco, F., Torres, T., Ortiz, J.E., 2010. La cueva de Gabasa revisada 15 años después: un cubil para las hienas y un cazadero para los neandertales. Zona Arqueológica 13, 376–389.

Vega Bolivar, S., Samper Carro, S.C., Pizarro, J., Mora, R., Martinez-Moreno, J., Benito-Calvo, A., 2018. Abric Pizarro (Ager, Lleida): Un nou jaciment de Paleolitic mitja al Prepirineu Oriental. Prim. Jornades Arqueol. Paleontol. Ponent 32–39.

Vidal-Matutano, P., Henry, A., Théry-Parisot, I., 2017. Dead wood gathering among Neanderthal groups: charcoal evidence from Abric del Pastor and El Salt (Eastern Iberia). J. Archaeol. Sci. 80, 109–121.

Villa, P., Mahieu, E., 1991. Breakage patterns of human long bones. J. Hum. Evol. 21, 27–48.

Villa, P., Roebroeks, W., 2014. Neanderthal demise: an archaeological analysis of the modern human superiority complex. PLoS One 9, e96424.

Westbury, E., Samper Carro, S.C., Vega Bolivar, S., Pizarro, J., Martínez-Moreno, J., Mora, R., 2024. Neanderthal resilience and adaptability: insights from the Abric Pizarro faunal assemblage during the MIS 4. Frontiers in Environmental Archaeology - Zooarchaeology 3, 1–25. https://doi.org/10.3389/fearc.2024.1405535.

White, T.D., 1992. Prehistoric Cannibalism at Mancos. Princeton University Press, Princeton.

Yravedra, J., Cobo-Sánchez, L., 2015. Neanderthal exploitation of ibex and chamois in southwestern Europe. J. Hum. Evol. 78, 12–32.

Zhou, H., Zhao, J., Qing, W., Feng, Y., Tang, J., 2011. Speleothem-derived Asian summer monsoon variations in Central China, 54–46 ka. J. Quat. Sci. 26 (8), 781–790.

Zilhão, J., Angelucci, D.E., Araújo Igreja, M., Arnold, L.J., Badal, E., Callapez, P., Cardoso, J.L., d'Errico, F., Daura, J., Demuro, M., Deschamps, M., Dupont, C., Gabriel, S., Hoffmann, D.L., Legoinha, P., Matias, H., Monge Soares, A.M., Nabais, M., Portela, P., Queffelec, A., Rodrigues, F., Souto, P., 2020. Last interglacial Iberian Neandertals as Fisher-hunter-gatherers. Science 367, 6485.

Zilhão, J., Angelucci, D.E., Arnold, L.J., d'Errico, F., Dayet, L., Demuro, M., Deschamps, M., Fewlass, H., Gomes, L., Linscott, B., Matias, H., Pike, A.W.G., Steier, P., Talamo, S., Wild, E.M., 2021. Revisiting the middle-to-upper palaeolithic transition at Gruta do Caldeirão (Tomar, Portugal). PLoS One 16 (10), e0259089. https://doi.org/10.1371/journal.pone.0259089.